UNCLASSIFIED

REPORT DOCUMENTATION PAGE	READ INSTRUCTIONS BEFORE COMPLETING FORM

1. REPORT NUMBER	2. GOVT ACCESSION NO.	3. RECIPIENT'S CATALOG NUMBER
DTNSRDC-ASED-CR-1-82	AD-A111 278	

4. TITLE (and Subtitle)	5. TYPE OF REPORT & PERIOD COVERED
Analytical Investigation of High Performance, Short, Thrust Augmenting Ejectors	Report on Theoretical Phase April 1980 – April 1981
	6. PERFORMING ORG. REPORT NUMBER
	Aero Report/1274/CU-ME-F-1-81

7. AUTHOR(s)	8. CONTRACT OR GRANT NUMBER(s)
Tah-teh Yang and Francois Ntone	DTNSRDC Research Contract N00167-80-C-0040

9. PERFORMING ORGANIZATION NAME AND ADDRESS	10. PROGRAM ELEMENT, PROJECT, TASK AREA & WORK UNIT NUMBERS
Mechanical Engineering Department Clemson University Clemson, SC 29631	Task Area 9R023-02 Work Unit 1-1606-300

11. CONTROLLING OFFICE NAME AND ADDRESS	12. REPORT DATE
David W. Taylor Naval Ship R&D Center Aviation and Surface Effects Department Bethesda, MD 20084	January 1982
	13. NUMBER OF PAGES
	69

14. MONITORING AGENCY NAME & ADDRESS(if different from Controlling Office)	15. SECURITY CLASS. (of this report)
	UNCLASSIFIED
	15a. DECLASSIFICATION/DOWNGRADING SCHEDULE

16. DISTRIBUTION STATEMENT (of this Report)

APPROVED FOR PUBLIC RELEASE: DISTRIBUTION UNLIMITED

17. DISTRIBUTION STATEMENT (of the abstract entered in Block 20, if different from Report)

18. SUPPLEMENTARY NOTES

19. KEY WORDS (Continue on reverse side if necessary and identify by block number)

Contour Wall Diffuser
Ejector
Thrust Augmenting Ejector
High Performance Ejector

20. ABSTRACT (Continue on reverse side if necessary and identify by block number)

A procedure for analyzing thrust augmenting ejectors having a short, curved-wall diffuser is presented. In this type of diffuser a shear flow is admitted at the inlet and a set of auxiliary ejectors is used to provide the necessary boundary layer control. Several computer programs are used in the analytical procedure. These computer programs are either outlined or referenced in the open literature. A user's manual is provided in the Appendices of this report. A discussion of the geometries and performances, including thrust

DD FORM 1 JAN 73 1473 EDITION OF 1 NOV 65 IS OBSOLETE
S/N 0102-LF-014-6601

UNCLASSIFIED

augmentation ratios, of two sample ejectors determined by use of this analytical procedure with mixing chamber contraction as an optimization parameter is presented. Use of the mixing chamber length as an optimization parameter is also discussed.

TABLE OF CONTENTS

LIST OF FIGURES

NOMENCLATURE

A	Cross-sectional area
AR	Ejector exit to inlet area ratio
AR	Diffuser area ratio
B	Nondimensional vorticity
C	Dimensional constant describing the amount of contraction of the mixing chamber
C_p	Specific heat at constant pressure
D	Mixing chamber diameter at inlet
L	Mixing chamber length
$\dot{m}$	Mass flow rate
$\dot{m}_2$	Mass flow rate at diffuser exit
$\dot{m}_3$	Mass flow rate at exit of auxiliary ejector
$\dot{m}_p$	Mass flow rate of primary fluid in main ejector
$\dot{m}_{p'}$	Mass flow rate of primary fluid in auxiliary ejector
M_i	Mach number at diffuser inlet
MR	Ratio of secondary flow rate to primary flow rate in main ejector
MR_{aux}	Ratio of secondary flow ratio to rimary flow rate in auxiliary ejector
P	Local static pressure
P_{01}	Plenum chamber pressure
P_1	Static pressure at mixing chamber inlet
P_e	Static pressure at diffuser exit
P_i	Static pressure at diffuser inlet
$P r$	Prandtl number
Pr_t	Turbulent Prandtl number
q	Magnitude of velocity
r	Local radius of mixing chamber. Radial coordinate.

R	Radius of diffuser
$R_{e,diff}$	Radius of diffuser at its exit
$R_{e,mc}$	Radius of mixing chamber at its exit
$R_{in,mc}$	Radius of mixing chamber at its inlet
t	Time
T	Mean temperature
u	Mean axial velocity component in turbulent flow. Axial component of velocity in rotational flow.
u_{cr}	Velocity level below which all boundary layer fluid must be removed to avoid separation
U_1	Velocity at boundary layer edge, upstream of the slot
U_2	Velocity at boundary layer edge, downstream of the slot
v	Radial component of velocity
V_2	Average velocity at diffuser exit
V_3	Average velocity at exit of auxiliary ejector
V_p	Average velocity of primary fluid in main ejector
$V_{p'}$	Average velocity of primary fluid in auxiliary ejector
x	Axial coordinate
y	Radial distance from wall where the flow velocity is equal to u_{cr}
β	Correction factor accounting for non-uniform velocity distribution
γ	Ratio of specific heats
ϵ	Eddy viscosity
λ	Ratio of secondary area to primary area at ejector inlet
μ	Viscosity
ν	Kinematic viscosity
ω	Vorticity
ρ	Gas density
ϕ_1	Thrust aumentation ratio with $m_3 = m_p = 0$ in equation (16)

ϕ_2 Thrust augmentation ratio accounting for auxiliary ejector

ψ Stream function

χ Streamwise coordinate

ANALYTICAL INVESTIGATION OF HIGH PERFORMANCE,
SHORT, THRUST AUGMENTING EJECTORS

Tah-teh Yang and Francois Ntone
Mechanical Engineering Department, Clemson University
Clemson, South Carolina

ABSTRACT

A procedure for analyzing thrust augmenting ejectors using a short, curved-wall diffuser is presented. In this type of diffuser a shear flow is admitted at the inlet and a set of auxiliary ejectors is used to provide the necessary boundary layer control. Several computer programs are used in the analytical investigation. Analyses of these computer programs are either outlined or referenced in the open literature. A user's manual is provided in the appendices of this report. A discussion of the geometries and performances, including thrust augmentation ratios, of two sample ejectors determined by use of the present analysis procedure with mixing chamber contraction as an optimization parameter is presented. Use of the mixing chamber length as an optimization parameter is also discussed.

ADMINISTRATIVE INFORMATION

1. INTRODUCTION

The thrust augmentation ratio of an ejector depends to a large degree on the effectiveness of its diffuser (1, 2, 3). In early 1970 Yang and El-Nasher

(4) carried out an exploratory investigation with an ejector having a short curved-wall diffuser. They used saturated steam for the primary flow and ambient air as the secondary flow. Their objective was to examine the potential increase in ratio of the mass flow rate at the ejector exit to the primary flow at the nozzle exit. The pressure ratio range of their experiments was 40 to 400*. On the average the mass ratios were more than twice those reported by Hickman (5). In Yang and El-Nashar's experiments a centrifugal pump provided the boundary layer control for the short curved-wall diffuser, and the rate at which the fluid was removed from the boundary layer was less than 15% of the total flow rate at the exit of the ejector or the diffuser. Based on the mass flow rate and the velocity profiles at the diffuser exit, a maximum thrust augmentation ratio of 2.81 was estimated. The high value of the thrust augmentation ratio is partly attributed to the use of steam as the primary flow. This value would have been approximately 2 if air of the same stagnation pressure but of a lower stagnation temperature had been used for the primary flow. However, the most important feature of this ejector is its overall length. Because a short curved-wall diffuser was used, the length of the ejector was reduced to about one-half the length of a conventional ejector. This reduction in length is particularly attractive for application where the length restriction is severe. The disadvantage of such an ejector is the need for boundary layer control. A scheme for using a set of secondary nozzles to form an auxiliary ejector and thus to provide the necessary boundary layer control was evolved. The discharge from this auxiliary ejector is oriented in the same direction as the main ejector and therefore contributes to the overall thrust; this makes the use of boundary layer control more acceptable. Figure 1 shows a sketch of a thrust augmentor equipped with a short curved-wall diffuser where a set of secondary jets provide boundary layer suction for the diffuser.

The short curved-wall diffuser was developed at Clemson University during the late 1960s and early 1970s. Details of the analytical and experimental flow fields within these diffusers have been reported in engineering journals

---

* Following jet pump convention, this pressure ratio is defined as $(P_{01}-P_e)/(P_e-P_1)$.

(6, 7, 8, 9, 10), as well as in contractor reports (11, 12, 13, 14). These diffusers, designed by using the Inverse Method, have sometimes been referred to in the literature as Griffith diffusers because the velocity distribution along the diffuser wall is taken from the high lift airfoil designed by A. A. Griffith in 1938. A typical Griffith Diffuser wall velocity distribution is shown in Figure 2. It exhibits a high velocity inlet region, slightly accelerating flow up to a narrow region, and a sudden drop in velocity across a narrow slot region. Downstream of the slot region there is an exit region toward the end of the diffuser. Figure 3 shows the typical shape of the diffuser which is the result of the prescribed wall velocity distributions. Figure 4 shows several velocity distributions of the potential flow along the streamlines away from the diffuser wall.

Since there is no deceleration over the solid surface, flow separation cannot take place. However, if fluid is to jump over the slot region, it must have a velocity higher than the critical velocity. The critical velocity can be computed by using Taylor's criterion (15). Much experimental data have been examined for diffuser inlet flows having thin boundary layers with core flows well represented by potential flow theory. In such cases, experimentally obtained wall pressure distributions agree with the theoretically prescribed distributions. In ejectors, however, the diffuser inlet flow is significantly different from irrotational flow.

Based on the inlet velocity measurements reported by Hill and Gilbert (16), it appears that the diffuser inlet flow should be represented by a shear flow of uniform vorticity. Under this condition (admitting a shear flow) the wall pressure distribution could be significantly different from that which was prescribed for the particular diffuser. Specifically, this raises a concern about the presence of an adverse pressure gradient or a deceleration in diffuser wall velocity which may result from the inlet shear flow. A moderate deceleration upstream of the suction slot may be overcome by increasing the suction flow rate. A strong deceleration will result in flow separation. The combination of a large design area ratio and inlet vorticity could also create a flow reversal at the diffuser exit because of the shear flow requirement, even in an inviscid flow. It becomes apparent, therefore, that a method of

calculating the wall velocity of a rotational flow in this type of curved diffuser is necessary to assure that there will be no adverse pressure gradient along the diffuser wall. This will allow us to obtain the high thrust augmentation thrust augmentation benefit afforded by using a short, curved-wall diffuser section in the ejector design.

2. ANALYSES

The analyses in this investigation will be presented in the order outlined in Figure 5.

2.1 MIXING CHAMBER GEOMETRY

The geometry of a mixing chamber is described by the equation

$$r = R_{in,mc} \left\{ 1 \frac{C}{R_{in,mc}} \tanh \left[5(\frac{x}{L})^2 - \frac{10}{3}(\frac{x}{L})^3 \right] \right\} \tag{1}$$

where r is the radius at any location of x

$R_{in,mc}$ is the radius of the mixing chamber at the inlet

$x = 0$ is the location of the mixing chamber inlet

$x = L$ is the location of the mixing chamber exit

C is a dimensional constant.

Thus, contraction is gradual and the maximum contraction takes place at the exit of the mixing chamber. This geometry provides zero wall slopes at the inlet and exit of the mixing chamber.

4

2.2 DTNSRDC EJECTOR PROGRAM

The DTNSRDC ejector program is a modification of Gilbert and Hill's ejector analysis program (16). It includes a new feature which can design a diffuser with the incipient separation criterion in which the skin friction velocity is maintained at a low non-zero value in the diffuser. This criterion produces faster pressure recovery in the diffuser, and therefore reduces the overall ejector length. The following boundary layer type momentum and energy equations were used in the DTNSRDC ejector program (17).

χ-Momentum

$$u \frac{\partial u}{\partial \chi} = \frac{ur}{2\psi} \frac{\partial}{\partial \psi} \left[(\mu + \epsilon) \frac{\rho ur}{2\psi} \frac{\partial u}{\partial \psi} \right] - \frac{1}{\rho} \frac{\partial P}{\partial \chi} \tag{2}$$

ψ-Momentum

$$\frac{\partial P}{\partial \psi} = 0 \tag{3}$$

Energy

$$u \frac{\partial (c_p T)}{\partial \chi} = \frac{u}{\rho} \frac{\partial P}{\partial \chi} + \frac{ur}{2\psi} \frac{\partial}{\partial \psi} \left[\left(\frac{\mu}{Pr} + \frac{\epsilon}{Pr_t} \right) \frac{\rho ur}{2\psi} \frac{\partial (c_p T)}{\partial \psi} \right]$$
$$+ \left(\frac{\mu + \epsilon}{\rho} \right) \left(\frac{\rho ur}{2\psi} \frac{\partial u}{\partial \psi} \right)^2 \tag{4}$$

The symbols in the equations are defined in the Nomenclature. These equations were solved using the finite difference method. A flow diagram for the computer program and instructions for input of data are reported in Appendix A.

The utilization of this program for the present study is limited to the determination of the velocity and temperature distribution up to the exit of the mixing chamber.

2.3 AVERAGE VELOCITY AND TEMPERATURE AT THE EXIT OF THE MIXING CHAMBER

The velocity and temperature are computed using the DTNSRDC Ejector Program and are printed out for all the selected streamlines at preselected stations. The pressure variations, however, are only considered along streamlines instead of across streamlines. Therefore the averaging process only deals with the mass averaged velocity and temperature. No pressure averaging is necessary. These averages are given by

$$(u)_{ave} = \frac{\int u\rho\, dA}{A(\rho)_{ave}} \tag{5}$$

and

$$(T)_{ave} = \frac{\int Tu\rho\, dA}{A(\rho)_{ave}(u)_{ave}} \tag{6}$$

2.4 DIFFUSER AREA RATIO, CURVED-WALL DIFFUSER GEOMETRY AND THE ROTATIONAL FLOW CALCULATIONS

2.4.1 <u>Diffuser Area Ratio</u> -- Using equations (5) and (6), the Mach number at the diffuser inlet, M_i, can be determined. The diffuser inlet pressure P_i is merely the pressure at the last station of the mixing chamber. Assuming the flow in the diffuser is isentropic, and the exit pressure P_e is the ambient pressure for the analysis, the following formula is used to calculate the diffuser area ratio AR.

$$AR = \left[\frac{\frac{\gamma-1}{2}\left(\frac{P_i}{P_e}\right)^2}{\left(\frac{1}{M_i^2} + \frac{\gamma-1}{2}\right)\left(\frac{P_i}{P_e}\right)^{\frac{\gamma-1}{\gamma}} - \frac{1}{M_i^2}} \right]^{1/2} \tag{7}$$

2.4.2   The Curved-Wall Diffuser Geometry -- The geometry of the curved-wall diffuser is determined by using the "Clemson Inverse Design Program for Short Curved-Wall Diffusers." Reference 13 provides the necessary instructions for input data preparations. For plane-flow cases, Griffith diffusers can be designed by specifying only the area ratio, length-to-exit diameter ratio, and the percentage of flow removal used for boundary layer control (18). For axisymmetric diffusers the current version of the computer program requires input of the stream function and the velocity potential at the boundary. An educated guess of input values is helpful.

2.4.3   Rotational Flow Calculations -- First we examine the complete vorticity equation in vectorial form as follows:

$$\frac{\partial \vec{\omega}}{\partial t} + (\vec{u} \cdot \vec{\nabla})\vec{\omega} = (\vec{\omega} \cdot \vec{\nabla})\vec{u} + \nu \nabla^2 \vec{\omega} \tag{8}$$

Consistent with the approximations made in this study, the viscosity term is neglected and therefore:

$$\frac{\partial \vec{\omega}}{\partial t} + (\vec{u} \cdot \vec{\nabla})\vec{\omega} = (\vec{\omega} \cdot \vec{\nabla})\vec{u} \tag{9}$$

For axisymmetric flow, the term $(\vec{\omega} \cdot \vec{\nabla})\vec{u}$ is equal to $\frac{v\omega}{r}$. For $\frac{v}{u} \ll 1$, $(\vec{\omega} \cdot \vec{\nabla})\vec{u} \approx 0$ and consequently

$$\frac{D\vec{\omega}}{Dt} \approx 0 \tag{10}$$

or vorticity is approximately constant throughout the diffuser.

The continuity equation for incompressible axisymmetric flow is:

$$\frac{\partial v}{\partial r} + \frac{\partial u}{\partial x} + \frac{v}{r} = 0 \tag{11}$$

Figure 6 defines the coordinate system and the velocity components used in the analysis.

7

The stream function $\psi(r,x)$ is defined such that:

$$u = \frac{1}{r} \frac{\partial \psi}{\partial r} \quad \text{and} \quad v = -\frac{1}{r} \frac{\partial \psi}{\partial x} \tag{12}$$

and then equation (11) becomes:

$$\frac{1}{r^2} \frac{\partial \psi}{\partial x} - \frac{1}{r} \frac{\partial^2 \psi}{\partial r \partial x} + \frac{1}{r} \frac{\partial^2 \psi}{\partial x \partial r} - \frac{1}{r} \left(\frac{1}{r} \frac{\partial \psi}{\partial x} \right) = 0 \tag{13}$$

In addition, ψ satisfied the vorticity equation which in cylindrical coordinates for an axisymmetric shear flow is:

$$\frac{\partial v}{\partial x} - \frac{\partial u}{\partial r} = |\omega| \tag{14}$$

Substituting equation (12) in equation (14) yields

$$\frac{\partial^2 \psi}{\partial x^2} + \frac{\partial^2 \psi}{\partial r^2} = \frac{1}{r} \frac{\partial \psi}{\partial r} - |\omega| r \tag{15}$$

Which is an elliptic partial differential equation. In the numerical solution of equation (15) for rotational flow, we use the same grid network as for irrotational flow. The boundary conditions used are as follows.

2.4.3.1 Inlet -- At the diffuser inlet, there is a parallel flow in the x-direction, and consequently $v = 0$. The ψ's are obtained from equation (12) as follows

$$\frac{1}{r} \frac{\partial \psi}{\partial r} = u \quad \text{and} \quad -\frac{1}{r} \frac{\partial \psi}{\partial x} = 0$$

Therefore ψ only changes with r, hence

$$\frac{d\psi}{dr} = ur$$

For shear flow,

$$u = u_{o,in} - |\omega| r$$

8

therefore

$$\psi = \int_0^r r(u_{o,in} - \omega r)\,dr$$

Which yields

$$\psi = \frac{1}{2} r^2 u_{o,in} - \frac{1}{3} \omega r^3 \qquad (16)$$

From equation (16), we have:

$$\psi_{wall} = \frac{1}{2} R_{in}^2 u_{o,in} - \frac{1}{3} \omega R_{in}^3 \qquad (17)$$

where $R = r(\psi_{wall})$

For irrotational flow and uniform parallel inlet velocity q_{irr}, we have:

$$\psi_{irr} = \int_0^{R_{in}} r q_{irr}\,dr$$

At the wall:

$$(\psi_{irr})_{wall} = \frac{1}{2} q_{irr} R_{in}^2 \qquad (18)$$

However, ψ_{wall} may not necessarily be equal to $(\psi_{irr})_{wall}$, which means that for the same diffuser geometry, flow rates for the irrotational and rotational (shear) cases may not be the same.

Define γ such that

$$(\psi_{irr})_{wall} = \gamma \psi_{wall}$$

and then

$$q_{irr} = \gamma(u_{o,in} - \frac{2}{3} \omega R_{in}) \qquad (19)$$

9

For the shear flow solution, we will need to (i) specify, for the inlet boundary condition, the values of $u_{o,in}$ and γ; (ii) obtain ω from equation (19); and (iii) specify the streamline according to equation (16).

Another possibility is that both ω and $u_{o,in}$ are specified, and γ is to be calculated from equation (19).

In the inverse design program if we have prescribed parallel but non-uniform irrotational flows at the inlet and the exit, then the boundary condition at the inlet would be as follows:

$$(\psi_{irr})_{wall} = \gamma\left[\frac{1}{2} R_{in}^2 u_{o,in} - \frac{1}{3} \omega R_{in}^3\right]$$

For known ω and $u_{o,in}$, γ can be calculated from the following

$$\gamma = \frac{(\psi_{irr})_{wall}}{\frac{1}{2} R_{in}^2 u_{o,in} - \frac{1}{2} \omega R_{in}^3} \tag{20}$$

and the streamlines can be calculated from equation (16).

2.4.3.2   Centerline

Along the centerline, we have $\psi = 0$.

2.4.3.3   Wall, upstream of slot

Along the wall, upstream of the slot, we have $\psi = \psi_{wall}$, where ψ_{wall} is the same as the one calculated at the inlet.

2.4.3.4   Wall, downstream of slot and inside of slot

Let β and β_{irr} be the fractions of the flow into the slot for the rotational and irrotatonal cases respectively. These β's are related to the stream functions as shown in the following expressions.

10

$$\beta_{irr} = 1 - \frac{\psi_{irr,st}}{\psi_{irr,wall}} \tag{21}$$

and

$$\beta = \frac{\psi_{wall} - \psi_{st}}{\psi_{wall}}$$

or

$$\psi_{st} = \psi_{wall}(1 - \beta) \tag{22}$$

β is specified as an input to the analysis. The ψ values for lines AB and AC in Figure 7 are determined from equation (21).

2.4.3.5 Diffuser Exit

Letting Q_{irr} = Volumetric flow rate at the diffuser exit for irrotational flow and

Q = Volumetric flow rate at diffuser exit for shear flow results in:

$$Q_{irr}/(1 - \beta_{irr}) = \gamma Q/(1 - \beta) \tag{23}$$

It can be shown that for parallel flow

$$u_{o,e} = \frac{2}{3}\omega R_{NSTAGU} + \frac{2(\psi_{irr})_{wall}(1 - \beta)}{\gamma R_{NSTAGU}^2} \tag{24}$$

Here ω is specified, ψ_{irr} and R_{NSTAGU} are obtained from the Clemson Inverse Solution Computer Program, and $u_{o,e}$ is the center line velocity at the diffuser exit. (R_{NSTAGU} is the radius at the stagnation point A of Figure 7.)

2.4.3.6 Exit of Slot

At the slot exit, a shear flow having vorticity ω is assumed. Referring to Figure 8:

$$R - R_o = y \sin(90^\circ - \alpha) = y \cos \alpha$$

11

or

$$R = R_o + y \cos \alpha \tag{25}$$

The following development is to determine the stream function in the slot.

$$\psi_y - \psi_{st} = \int_o^y qRdy \tag{26}$$

But from Figure 9 we see that, $q = q_{o,sl} - \omega y$
and therefore

$$\psi_y = \psi_{st} + R_o q_{o,sl} \, y + \frac{1}{2}(q_{o,sl} \cos \alpha - R_o \omega)y^2 - \frac{1}{3}\omega y^3 \cos \alpha \tag{27}$$

The ψ's at the exit of the slot can be prescribed using equation (27) where y is replaced by $\dfrac{(R-R_o)}{\cos \alpha}$, viz.

$$q_{o,sl} = \frac{\beta\psi_{wall} + \frac{1}{2}R_o\omega\left(\dfrac{R_{w,sl}-R_o}{\cos\alpha}\right)^2 + \frac{1}{3}\omega\left(\dfrac{R_{w,sl}-R_o}{\cos\alpha}\right)^3\cos\alpha}{R_o\left(\dfrac{R_{w,sl}-R_o}{\cos}\right) + \frac{1}{2}\left(\dfrac{R_{w,sl}-R_o}{\cos\alpha}\right)^2\cos\alpha} \tag{28}$$

The details of computational methods suitable for this equation subject to the proper boundary conditions are reported in references 19 and 20. The change of flow velocity in the diffuser is much less than that in the mixing chamber, therefore in this part of the computation incompressible flow is assumed, even though a compressible flow approach is used in computing the diffuser area ratio.

12

2.5 CRITICAL VELOCITY AND SUCTION FLOW RATE

Using rotational flow analysis, the flow velocities U_1 and U_2 outside the boundary layer immediately upstream and downstream from the suction slot are determined. From Taylor's criterion (15) the critical velocity is determined by the following formula:

$$u_{cr} = U_1 \sqrt{1 - \left(\frac{U_2}{U_1}\right)^2} \tag{29}$$

The following expression is a good approximation for u_{cr}

$$u_{cr} = U_1 \sqrt{1 - \left(\frac{1}{(AR)_{diff}}\right)^2} \tag{30}$$

where AR_{diff} is the diffuser area ratio.

In this analysis it is necessary to use the boundary layer velocity profile at the exit of the mixing chamber to approximate the boundary layer velocity profile immediately upstream of the suction slot. Therefore the suction flow rate can be determined by computing the mass flow rate within the boundary layer up to the location where the flow velocity is equal to the critical velocity u_{cr}. This suction flow rate is computed as follows

$$\dot{m}_{suction} = 2\pi \int_{R_{e,mc}}^{R_{e,mc}-y} \rho u r\, dr \tag{31}$$

where y is the location where the flow velocity is equal to u_{cr}.

2.6 GLOBAL ANALYSIS FOR ϕ_2

The thrust augmentation ratio ϕ_2, which accounts for the primary flow in the auxiliary ejector and the thrust contribution of its discharge, is defined by

$$\phi_2 = \frac{\dot{m}_2 V_2 + \dot{m}_3 v_3}{\dot{m}_p V_p + \dot{m}_{p'} v_{p'}} \tag{32}$$

where $\dot{m}$ is mass flow rate. The subscripts 2 and 3 are for the ejector exit and auxiliary ejector exit, respectively, subscript p is for the primary flow of the nozzle, and subscript p' represents the primary flow at the auxiliary nozzles.

The Global analysis was performed at the beginning of this project and a one-dimensional compressible air-to-air system was assumed. The primary purpose of the Global Analysis was to examine the necessary performance levels of mass ratios in the main and auxiliary ejectors in order to pre-select a value of $\dot{\phi}_2$. Toward the end of the analytical investigation, we found that the Global analysis is useful in providing a ϕ_2 value with a geometry obtained by following analytical procedure steps 1 through 5 based on mass averaged velocity. The Global analysis is attached as Appendix B.

2.7 CORRECTION OF ϕ_2 FOR NON-UNIFORM VELOCITY

Both inlet and exit of the diffuser have uni-directional flows. With known vorticity at the diffuser inlet and the constraint of constant vorticity throughout the diffuser, the exit flow velocity across the diffuser can be readily computed. The relationship between a mass-averaged velocity and a momentum-averaged velocity can be calculated for a known non-uniform velocity distribution, thereby providing a correction for ϕ_2. The following is the formula for this correction factor,

14

$$\beta = \frac{A\int_0^{R_{e,diff}} u^2(y)\,dA}{\left(\int_0^{R_{e,diff}} u(y)\,dA\right)^2}$$

and the final value of the thrust augmentation is obtained as follows

$$(\phi_2)_{corrected} = \beta(\phi_2)_{global\ analysis}$$

3. ANALYTICAL PROCEDURES FOR INVESTIGATING AN EJECTOR WITH SHORT CURVED-WALL DIFFUSER

Figure 5 shows the major steps in analyzing an axisymmetrical ejector with a short, curved-wall diffuser. The mixing chamber is shaped like a circular pipe with a contraction toward the end of the mixing chamber. To initiate the analysis investigation, the area ratio of the primary nozzle to the mixing chamber inlet and the ratio of the mixing chamber length to its diameter (L/D) are specified. The diffuser length usually is restricted to about one exit diameter of the diffuser. In addition, the static pressure at the mixing chamber inlet and stagnation pressure of the primary air are also specified. Both the entrained secondary flow from the stagnant ambient and the primary flow within the nozzle are isentropic up to the mixing chamber inlet. Specifying the static pressure at the mixing chamber inlet in fact implies specifying the ratio of the secondary mass flow to the primary mass flow. Starting from the inlet, there is heat and momentum transfer between the primary flow and the entrained secondary flow.

The first step is to specify the mixing chamber geometry by a selected value of C along with other mixing chamber geometric parameters. In step 2, the DTNSRDC ejector program (17) is used to compute velocity and temperature profiles and pressure values up to the exit of the mixing chamber. Governing equations for the flow are of the boundary layer type; therefore pressure

15

variations only exist along the flow directions and not across the streamlines.

In the third step, the mass-averaged flow velocity and temperature are computed. In the fourth step, one-dimensional, compressible isentropic flow is assumed in determining the necessary area ratio to yield the diffuser exit pressure at the atmospheric level (or the ambient level). For other computations in this step, inviscid imcompressible axisymmetric flow is assumed within the diffuser. As long as the flow along the solid wall is maintained without deceleration, the inviscid flow approximation can be justified. Under the framework of this approximation the vorticity of the flow will remain constant everywhere in the diffuser. The Clemson Inverse Design Program (13) is used to obtain the geometry of the short curved-wall diffuser for a specified area ratio at a length approximately equal to one exit diameter. This length specification is somewhat arbitrary, yet experience suggests that it should not be difficult to achieve. Immediately after the determination of the diffuser geometry, a computer program from the analysis of "Method of Rotational Flow Calculation in Griffith Diffuser" (19) is used to examine the velocity distribution along the diffuser wall. It is essential that there be no deceleration along the solid diffuser wall. When necessary, the input for the Inverse Design Program is revised to generate a new diffuser geometry. This process is repeated until there is no deceleration a'ong the diffuser wall. It is sometimes necessary to revise the analysis from the very first step where the mixing chamber inlet pressure is specified. An increase of the static pressure at the inlet implies a reduction in mass ratio and therefore a reduction in diffuser area ratio. Usually this revision can eliminate the problem of deceleration along the solid wall. For a configuration with no deceleration, no flow separation will take place. It is recommended that the velocity from the diffuser inlet to the suction slot be kept slightly accelerated.

In order to estimate the amount of fluid to be removed by boundary layer control, it is necessary to know the boundary layer profile immediately upstream of the suction slot. It is reasonable to assume that this profile is

16

the same as that at the exit of the mixing chamber, and by using that profile to calculate the critical velocity determined by Taylor's criterion, the rate of boundary layer removal can be determined. This approximation is compatible with other approximations used throughout this analytical procedure. A more accurate computation of viscous flow within the diffuser would require the use of the Navier-Stokes equation because appreciable pressure gradients exist across the streamlines.

It is apparent that the quality of the boundary layer at the mixing chamber exit would be improved if the mixing chamber had a contraction toward its exit to provide acceleration. With a contraction a smaller amount of the fluid within the boundary layer would have velocity below the critical velocity. On the other hand, a contraction of the mixing chamber will increase the diffuser area ratio and therefore elevate the value of the critical velocity determined by Taylor's criterion. A particular combination of these two counteracting factors will lead to a minimum suction requirement to achieve the necessary boundary layer control. Therefore, this analytical procedure is formulated with mixing chamber contraction as the optimization parameter.

In step 6, the modified thrust augmentation ratio ϕ_2 is computed. The consideration of the mass flow of primary fluid used in auxiliary ejectors to provide the necessary boundary layer control and the thrust contribution from the discharge of the boundary layer removal are included in the definition of ϕ_2. A one-dimensional compressible flow analysis which assumes the mass ratios of the primary and auxiliary ejectors and computes the mass averaged velocity at various parts of the ejector and the momentum terms at the ejector exit, yields the thrust augmentation ratio ϕ_2.

In step 3 the velocity across the mixing chamber exit has been computed, and in step 4 an inviscid shear flow with constant vorticity within the diffuser has been approximated. Therefore, the velocity across the diffuser exit can be readily determined. The last step, Step 7, is to correct the ϕ_2 value from the Global Analysis by using the known velocity distribution across the diffuser exit.

17

4. RESULTS AND DISCUSSIONS

4.1 COMPUTATIONAL RESULTS

The following computations are in accordance with the work statements of the research contract. These calculations were carried out for the purpose of examining the validity of a set of steam-to-air ejector data and to provide specific information for ϕ_2 values over a range of ejector parameters of immediate interest.

4.1.1 Steam-to-Air Ejector Analysis Program

-- In the introduction section of this report, a maximum thrust augmentation ratio of 2.81 was cited as an estimated value from the experimental mass flow ratio and velocity profile data of reference 4. The analytical tools discussed in Section 2 were used to examine the experimental data of reference 4 in the following manner.

4.1.1.1 Computer Program Modifications

-- It is recognized that the Hill and Gilbert ejector computer program (16) was developed for ejectors using air as both primary and secondary fluids. Modifications in computer programs were necessary in order to allow steam to be specified as the primary fluid. The gas constants such as $\gamma = 1.4$ and $R = 53.35$ ft-lb$_f$/lbm°R for air were changed to $\gamma = 1.135$ and $R = 85.76$ ft-lb$_f$/lbm°R, and the Prandtl number was changed from 0.7 to 1.05 wherever they appear in the computer program for calculations involving primary flow. The turbulent Prandtl number was left unchanged. In addition, in the modified computer program the identities of streamlines were maintained and provisions were made to use the correct properties (such as Pr) for each streamline in the finite difference solutions.

4.1.1.2 Comparison of Thrust Augmentation

-- The ejector geometries used in this comparison have mixing chamber inlet diameters and nozzle discharge diameters the same as those used in reference 4. Those experiments were conducted with nozzle stagnation pressures of 10, 15, 20 and 30 psig, and saturated steam was the primary fluid.

18

The computational procedure of this comparison is outlined as follows:

First, the inlet radius and the length of the mixing chamber, the primary nozzle flow area, the stagnation pressure and temperature of the primary and secondary air, and the static pressure at the mixing chamber inlet are specified. Specifying the static pressure at the mixing chamber inlet is equivalent to specifying the secondary flow rate. The values of static pressure used in computations were taken from experimental data of reference 4. After these values were specified, the DTNSRDC ejector design computer program was used to provide the diffuser geometry. The diffuser obtained from DTNSRDC program was used instead of Clemson curved-wall diffuser because the viscous flow is assumed to be of boundary layer type. The geometries of Clemson diffusers have curvatures too large to be considered acceptable for a boundary layer flow. A computer program is available at Clemson to accept a curved-wall diffuser with a pressure jump; the limit on the pressure jump, however, is too severe to be of practical value.

Second, the modified Hill and Gilbert program is used with steam as the primary fluid and air as the secondary fluid. The geometry of this ejector is identical to the resulting geometry of the DTNSRDC design program. The stagnation temperature and pressure of the primary flow have the same values as those used in the DTNSRDC program. The static pressure of the secondary flow at the inlet of the mixing chamber, however, is no longer specified. A new mass flow ratio is obtained as a part of the output. In general this new mass ratio, using steam as the primary flow, is about 30 to 40 percent higher than the mass ratio of an air-to-air ejector obtained with the DTNSRDC design computer program. On the average this new mass ratio is about 20% higher than experimentally obtained values.

Finally, the new mass flow ratio obtained from the Hill and Gilbert program is used as input to the global analysis program to compute the thrust augmentation values with assumed suction rates and assumed mass ratios for the auxiliary ejector. In the global analysis the thrust augmentation ϕ_2 is defined as follows:

19

$$\phi_2 = \frac{\dot{m}_2 v_2 + \dot{m}_3 v_3}{\dot{m}_p v_p + \dot{m}_{p'} v_{p'}}$$

Figure 10 shows three sets of results comparing analyitcal and experimental values of thrust augmentation. Two of these sets represent the analytical results of thrust augmentation ϕ_2 versus stagnation pressure of the primary flow with suction flow rates of 5% and 10% and the mass ratios of 4, 5, and 6-to-1 for the auxiliary ejector. The remaining single curve was obtained by letting $\dot{m}_3 = \dot{m}_p = 0$ and $\dot{m}_2$ correspond to the case of 15% suction without a secondary ejector. This single curve can now be compared directly with the thrust augmentation values ϕ_1 which were derived from the measured mass flow ratio and the exit velocity traverse from the aforementioned experiments (4), viz., using

$$\phi_1 = \frac{\dot{m}_2 v_2}{\dot{m}_p v_p}$$

The comparison indicates that the experimental values are in reasonably good agreement with the analytical values.

4.1.2 <u>Rotational Flow Calculations</u> — Figure 11 represents an axisymmetric diffuser having an area ratio of 2.5-to-1. Figure 12 shows the velocty distributions along the diffuser walls. The circles denote the velocity distribution prescribed to the "Inverse Design Program" for irrotational flow, and the triangles represent the velocity distribution along the diffusers depicted in Figure 11. The second velocity distributions were computed for inlet shear flow having a nondimensional vorticity value B of 0.33, where velocity and length are normalized by inlet center line velocity and inlet width respectively. It is apparent that even though the prescribed diffuser wall velocity distribution upstream of the slot has a strong acceleration, the wall velocity distributions may experience aeceleration in the diffuser when a shear flow is admitted. In actual operation a flow separation would most likely take place.

Figure 13 shows three velocity distributions for the diffuser depicted in Figure 11; these are specifically for inlet non-dimensional vorticity values of 0.33, 0.5, and 0.65. There is a significant change in the magnitude of the velocities, but their gradients vary only slightly. As expected, larger vorticity results in more deceleration. The larger change of wall velocity

20

magnitude results from the assumption in our analysis that the diffuser center line velocity is kept constant, therefore the wall velocity decreases more when the inlet shear flow vorticity increases more. Judging from the distributions of this figure, a flow separation would likely take place in all three cases. Figure 14 shows the wall velocity distributions for the diffuser depicted in Figure 11, under the conditions of (i) admitting an inlet shear flow with a vorticity of 0.5 and (ii) three different suction rates. A suction rate of 5.6% was the design value. At a suction rate of 8.5%, the velocity gradient upstream of the slot has not improved significantly in comparison to the distribution resulting from the 5.6% suction flow. Perhaps none of these distributions will yield a fully attached flow throughout the diffuser.

Figure 15 shows a diffuser designed for irrotational flow and having an area ratio of 2.5-to-1 with its suction slot slightly modified. Figure 16 shows the rotational velocity distribution along the walls of diffusers depicted in Figures 11 and 15 with inlet vorticity of 0.5. Apparently, there is no significant difference in wall velocity distribution for these two shear flow inlet cases. Figure 17 shows a diffuser designed for irrotational flow and having an area ratio of 2-to-1. Figure 18 shows wall velocity distribution for the diffuser dipicted in Figure 17. The velocity distribution represented by circles is for irrotational flow, and that represented by triangles is for shear flow with vorticity of 0.5. In this case hardly any deceleration is detected for the rotational flow, therefore, one should expect a highly effective diffuser even when a shear flow inlet condition is imposed at the curved wall diffuser inlet. Figures 19 and 20 are similar to Figures 17 and 18 and are for an area ratio of 1.5-to-1.

4.1.3 <u>Results from Parametric Study</u> -- The parametric study of thrust augmentation ratio ϕ_2 for an air-to-air ejector was made for a set of selective values with MR=12, $(MR)_{aux}$ = 4, F.S. = 0.10 and λ = 40. The mixing chamber has no contraction and its radius is 1.4 inches. The diffuser area ratios are around 2.0, which are the required values to provide the exit pressure level to match the ambient. The reasons for selecting these values are given in the section 4.2 of this report. The remaining parameters, $(L/D)_{overall}$ and P_{01}/P_1, were each varied from 2.5 to 5.0 in increments

21

of 0.5. The diffuser length was designed for one mixing chamber diameter approximately, therefore the mixing chamber length varied from 1.5 D to 4.0 D. The ejector inlet static pressure was slightly below the atmospheric pressure, therefore the nozzle stagnation pressure varied from 35 to 73 psia, approximately. The procedure used to calculate ϕ_2 is descirbed in section 3, the analytical procedure.

The results of this parametric study are presented in Figure 21 as ϕ_2 versus p_{oI}/p_I with $(L/D)_{overall}$ as parameter. Figure 21 shows that ϕ_2 increases with an increase of the pressure ratio and also increases with a decrease in length-to-diameter ratio, when the velocity at the nozzle exit was assumed to be sonic. The shaded area indicates the region where the vorticity at the diffuser inlet is too high for rotational flow to maintain a constant or a favorable pressure gradient along the curved-wall diffuser. For a short curved-wall diffuser to have attached flow, this requirement must be fulfilled. The computed ϕ_2 value will no longer be meaningful when the flow within the diffuser is separated. References 19 and 20 show that the non-dimensional vorticity should be kept below 0.8 for $(AR)_{diff}=2$. Therefore only 13 of the 36 cases computed in this investigation should be considered. Figure 22 shows the corrected ϕ_2 values, taking into account the difference between mass-averaged velocity and momentum-averaged velocity. Only the ϕ_2 values corresponding to those 13 cases for which the vorticity is less than 0.8 are presented.

Allowing the primary flow at the nozzle exit to reach supersonic speed, the ϕ_2 values will reduce to the levels as depicted in Figure 23. The trend of thrust augmentation versus pressure ratio exhibited in Figure 23 is in agreement with the traditional trend.

4.2 SAMPLE EJECTORS

Using the procedure outlined in Section 3, two sample ejectors were designed. These two ejectors may be candidates for future experimental investigation. Figure 24 shows one of the sample ejectors. First the primary nozzle diameter was selected. A diameter of 0.448 inches was chosen, based on

22

the capacity of a compressed air system in the Mechanical Engineering Department at Clemson University.

Next the design specification λ for the area ratio of the mixing chamber to the primary nozzle was selected. This ratio is somewhat limited by the amount of space available in a particular application. Since this thrust augmentation may have application in VSTOL aircraft, relatively smaller values, specifically 40 and 20, were used in comparison with the λ values of reference 4.

Based on the above specifications, the mixing chamber inlet diameters are 2.8 inches and 2.0 inches for $\lambda = 40$ and 20, respectively, and each mixing chamber has a 10% area reduction for contraction at its exit. The ratio of length of the mixing chamber to its inlet diameter, L/D, was selected to be 4. This length is not an optimum choice but is judged to be adequate and short enough not to be deemed excessive when considering viscous dissipation. A more adequate discussion will be given in this regard in the section 4.3 on the optimization process.

The diffuser area ratios are 2.187 and 1.993 for $\lambda = 40$ and 20, respectively. The corresponding ratios of overall length to mixing chamber inlet diameter are 5.256 and 5.182, and mass ratios of 12-to-1 and 7-to-1 are predicted with specified mixing chamber inlet static pressure levels.

The corresponding ϕ_2 values with the corrections for non-uniform diffuser exit velocities are predicted to be 1.50 and 1.30 for $\lambda = 40$ and 20, respectively, providing that a mass ratio of 4-to-1 is accomplished in the auxiliary ejectors for boundary layer control. In the literature, A. E. Kroll (3) reports that a mass flow ratio of 3 to 5-to-1 can be achieved with conditions similar to those of the auxiliary ejector. Using the DTNSRDC Ejector Program with the above mixing chambers, these values of mass ratio, 12-to-1 and 7-to-1, were shown to be possible with diffusers designed with the incipient separation criterion.

23

4.3 OPTIMIZATION

Using the mixing chamber contraction to optimize the thrust augmentation ratio was discussed in Section 3 on the analytical procedure. Figure 25 shows the fraction of suction required for necessary boundary layer control for MR = 12 and λ = 40. Figure 26 shows the estimated thrust augmentation ratios ϕ_2 for these specifications. The ϕ_2 increases slightly from 0% contraction to 10% contraction. For contractions of 10% to 15%, the ϕ_2 values are virtually constant, but a rapid decrease occurs beyond 20% contraction. A greater degree of contraction will produce a larger area ratio for the diffuser and may make it difficult to maintain non-deceleration along the diffuser wall. Therefore the optimum contraction is around 10%. The results for ejectors of MR = 7 and λ = 20 are similar. A slight increase in ϕ_2 was observed from 0% to 10% contraction. Beyond 15% contraction, decreases in ϕ_2 are observed due to a rapid increase in the required suction flow rate.

Optimization also can be applied to the mixing chamber length in the same way. It was found that for MR = 12 and λ = 40, ϕ_2 would increase from 1.50 to 1.63 if the mixing chamber length is 8.4 inches instead of the current design of 11.2. The reduction of the mixing chamber length will not only result in a decrease of boundary layer thickness, but also cause an increase of vorticity of the shear flow at the diffuser inlet. The second effect makes the maintenance of non-decelerating wall velocity more difficult. These two counteracting factors make the optimization process for length possible.

5. CONCLUSIONS

The major conclusions which were obtained from this investigation are:

1. Analysis shows that a significant increase in the thrust augmentation ratio of the thrust ejector can be achieved with significantly reduced overall length when a Griffith diffuser is used. Auxiliary jets to provide the necessary boundary layer control seem attractive because they are compact and simple in structure. Their effectiveness as a means of boundary layer control remains to be demonstrated experimentally.

24

2. In contrast to the irrotational flow case, for each value of vorticity there is an upper limit for the area ratio within which the diffuser can be designed without wall deceleration.

3. Reducing the diffuser area ratio is the most effective way to avoid deceleration along the diffuser wall. This implies that the initially specified mass flow rate of the primary ejector must be reduced.

4. Both the mixing chamber length and a contraction at the mixing chamber exit can be used as optimization parameters for thrust augmentation ratio.

6. REFERENCES

1. Porter, J. L., and Squyers, R. A., "A Summary/Overview of Ejector Augmentor Theory and Performance", Vought Corporation Advanced Technology Center, ATC Report No. R-91100-CR-47, April, 1981.

2. McClintock, F. A., and Hood, J. H., "Aircraft Ejector Performance", Journal of the Aeronautical Sciences, November, 1946.

3. Kroll, A. E., "The Design of Jet Pumps", Chemical Engineering Progress, February, 1947.

4. Yang, T., and El-Nasher, A. M., "Ejector Performance with a Short Diffuser", Proceedings of the Symposium on Jet Pumps and Ejectors, The British Hydromechanism Research Association, England, November, 1972.

5. Hickman, K. E., Gilbert, G. E., and Carey, J. H., "Analytical and Experimental Investigation of High Entrainment Jet Pumps", NASA CR-1602, 1970.

6. Nelson, C. D., Yang, T., and Hudson, W. G., "The Design and Performance of Axially Symmetric Contour Diffusers Employing Suction Boundary Layer Control", Journal of Engineering for Power, January, 1975.

7. Nelson, C. D., and Yang, T., "Inverse Problem Design Method for Branched and Unbranched Axially Symmetric Ducts", AIAA Journal, September, 1977, pp 1272-1277.

8. Yang, Tah-teh, "Comparison of High Performance Diffusers", Proceedings of the 6th Symposium of Turbomachinery, Tokyo, May, 1979, pp 30-36.

9. Yang, Tah-teh, and Nelson, C. D., "Griffith Diffusers," Journal of Fluids Engineering, December, 1979, pp 473-477.

10. Yang, Tah-teh, "Discussion on Griffith Diffusers", Journal of Fluids Engineering, June, 1980, p 248.

References cont.

11. Yang, Tah-teh, and Hudson, W. G., "Proposed Design and Experimental Performance of Short Two-Dimensional Curved Wall Diffusers Utilizing Suction Slots", NASA CR-120783, March, 1971.

12. Yang, Tah-teh, Hudson, W. G., and El-Nasher, A. M., "An Improved Method and Experimental Performance of Two-Dimensional Curved Wall Diffusers", NASA CR-121024, November, 1972.

13. Yang, Tah-teh, Hudson, W. G., and Nelson, C. D., "Design Method and Performance of Axially Symmetrical Short Diffusers", NASA CR-2209, March, 1973.

14. Yang, Tah-teh, Gaddis, J. L., and Chien, H. C., "Investigation of a Ramjet Using Boundary Layer Bleed in a Two-Dimensional Short Curved-Wall Subsonic Diffuser", Wright Patterson Air Force Base Technical Report, AFAPL TR-76-62, 1976.

15. Gregory, N., "Note on Sir Geoffrey Taylor's Criterion for the Rate of Boundary Layer Suction at a Velocity Discontinuity", R&M No. 2496, 1947.

16. Gilbert, G. B., and Hill, P. G., "Analysis and Testing of Two-Dimensional Slot Nozzle Ejectors with Variable Area Mixing Sections", NASA CR-2251, May, 1973.

17. Tai, T. C., "Optimization of Axisymmetric Thrust Augmenting Ejectors", AIAA Paper 77-707, June 1977.

18. Chien, H. C., "One-Step Method for Design of Griffith Diffusers", (Two-Dimensional), M.S. Thesis, Mechanical Engineering Department, Clemson University, 1976.

19. Ntone, F., "Method of Rotational Flow Calculations in a Griffith Diffuser", M.S. Thesis, Mechanical Engineering Department, Clemson University, 1981.

20. Yang, Tah-teh, and Ntone, Francois, "Rotational Flow In a Curved-Wall Diffuser Designed by Using the Inverse Method of Solution of Potential Flow Theory", Proceedings of 12th U.S. Navy Symposium on Aeroballistics, Bethesda, MD, May 12-14, 1981.
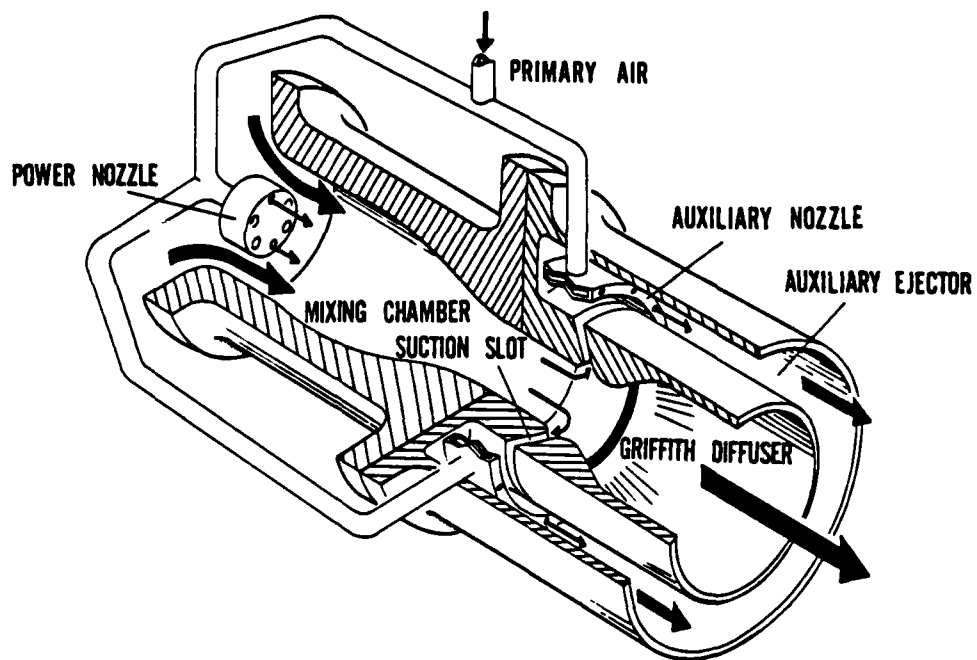
27

7. FIGURES

Figure 1. A sketch of a thrust augmentor with short curved-wall diffuser. Secondary jets are used to provide the necessary boundary layer control.
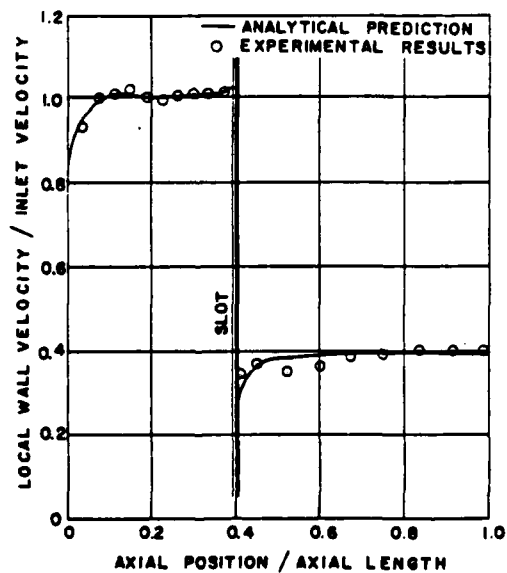

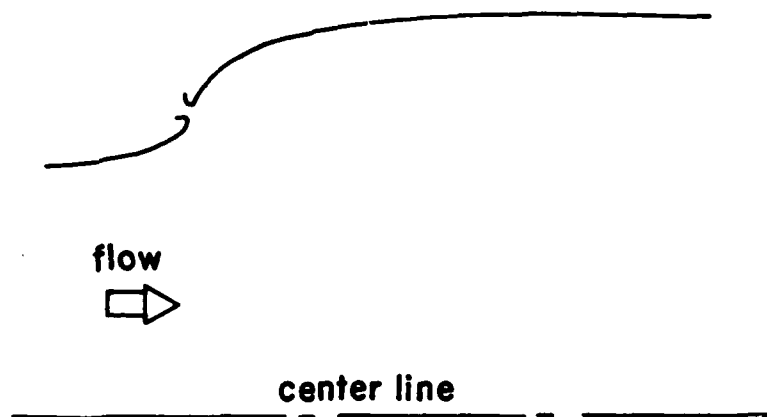Figure 2. Typical velocity distribution in a Griffith Diffuser.

29

flow ⇨
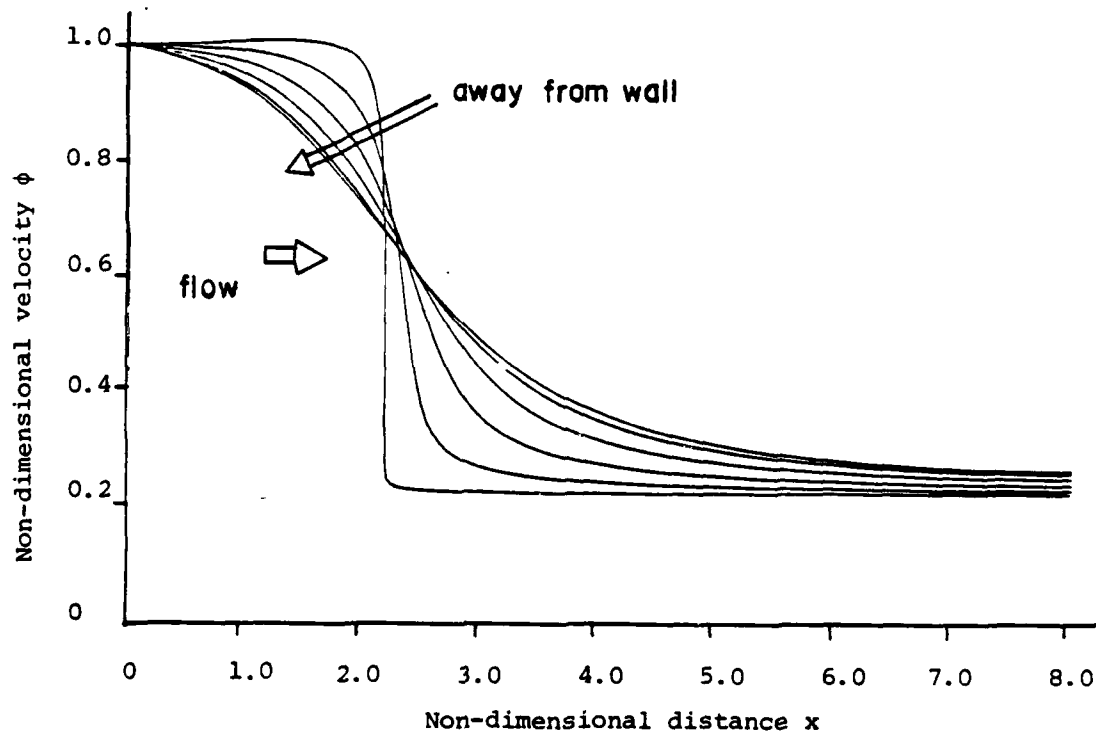
center line

Figure 3. Typical wall contour of a Griffith Diffuser.

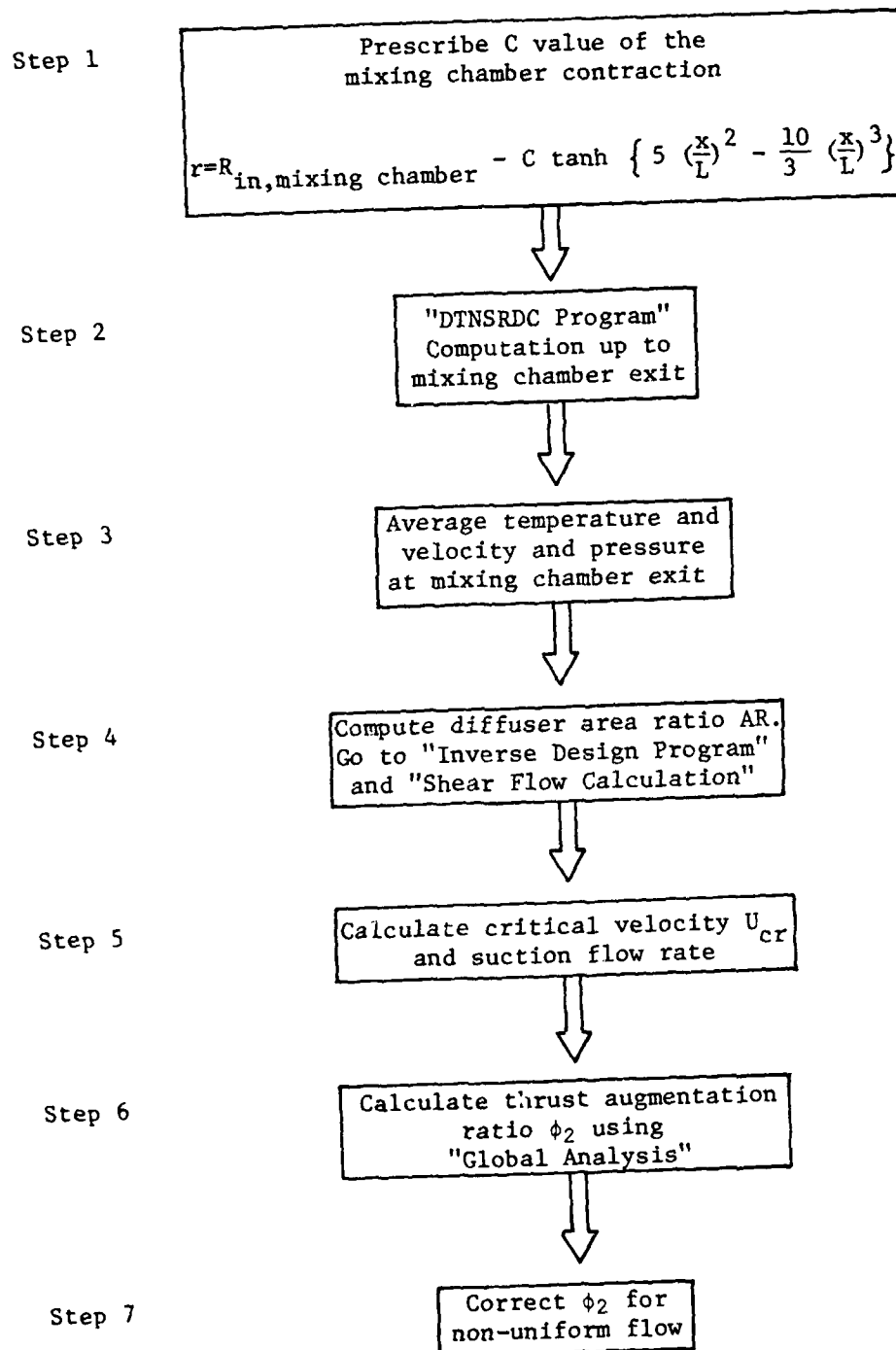Figure 4. Typical velocity variation along the streamlines
across the diffuser

30

Step 1	Prescribe C value of the mixing chamber contraction

$$r = R_{in,\text{mixing chamber}} - C \tanh \left\{ 5 \left(\tfrac{x}{L}\right)^2 - \tfrac{10}{3} \left(\tfrac{x}{L}\right)^3 \right\}$$

Step 2	"DTNSRDC Program" Computation up to mixing chamber exit

Step 3	Average temperature and velocity and pressure at mixing chamber exit

Step 4	Compute diffuser area ratio AR. Go to "Inverse Design Program" and "Shear Flow Calculation"

Step 5	Calculate critical velocity U_{cr} and suction flow rate

Step 6	Calculate thrust augmentation ratio ϕ_2 using "Global Analysis"

Step 7	Correct ϕ_2 for non-uniform flow

Figure 5. Block-diagram showing the major steps in ejector analysis.

31
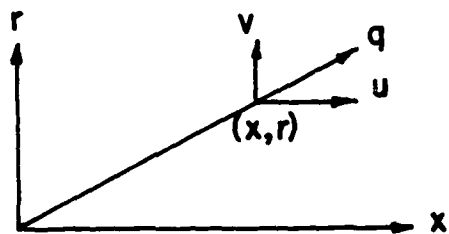
Figure 6. Coordinate system and velocity components used in analysis.
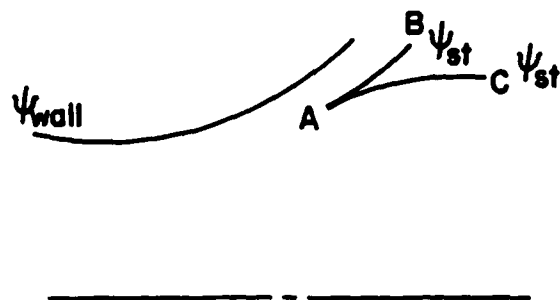
Figure 7. Wall streamlines and the branching point.
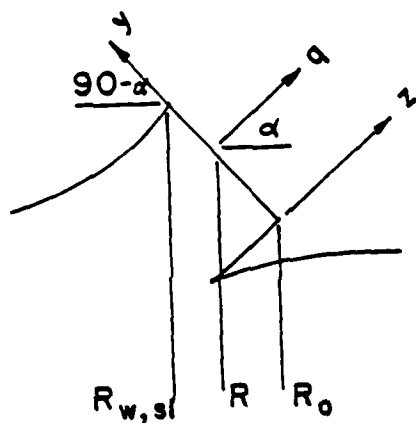

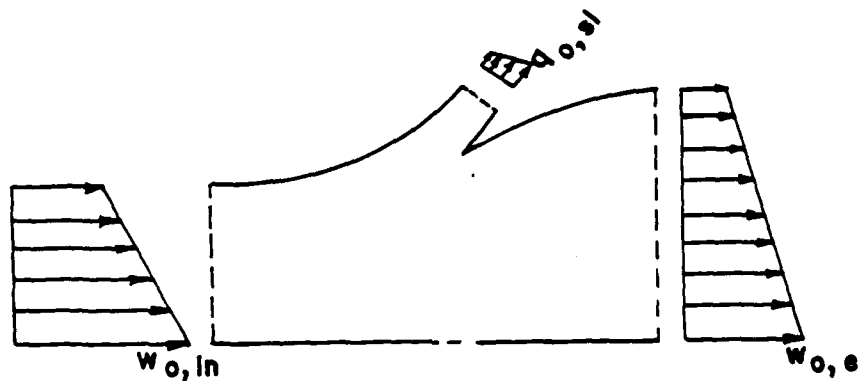Figure 8. Coordinate system at slot exit.

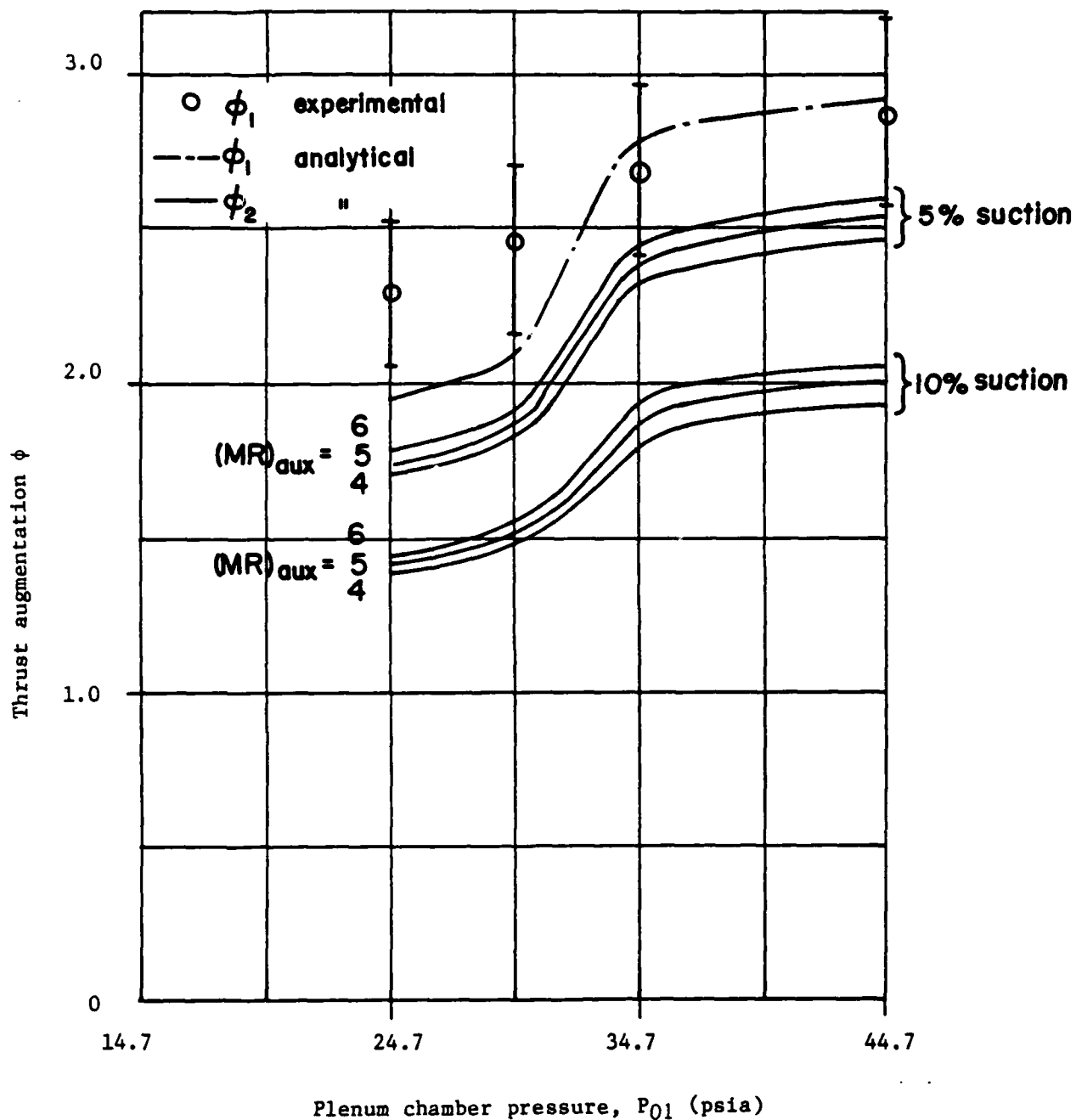Figure 9. Velocity distributions for shear flow.

Figure 10. A comparison of thrust augmentation ratio obtained analytically and obtained from experimentally measured mass ratio and velocity data. (Estimated error in ϕ_1 derived from experimental data $\pm$ 10%.)
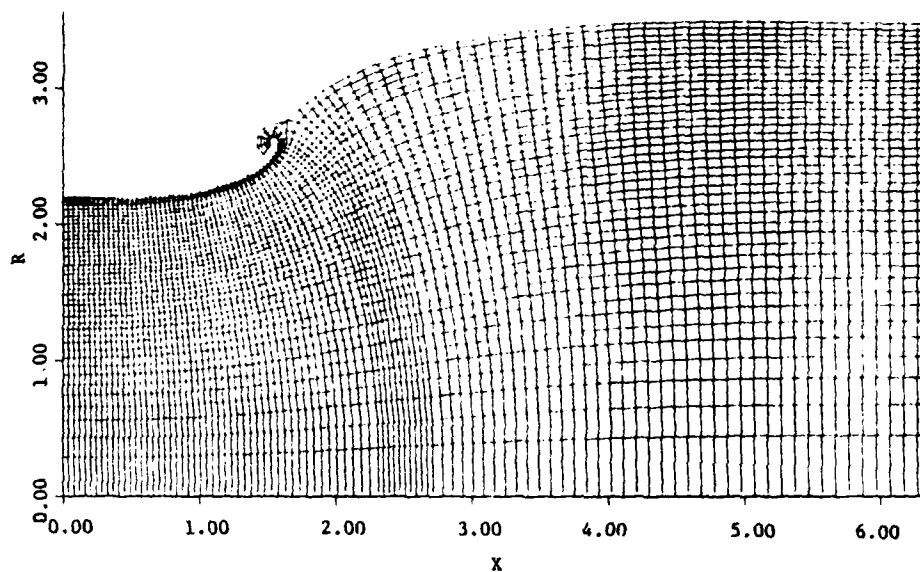
33

Figure 11. Computer plot of $\phi - \psi$ grid for an axisymmetric diffuser, AR = 2.5, suction rate = 5.6%.
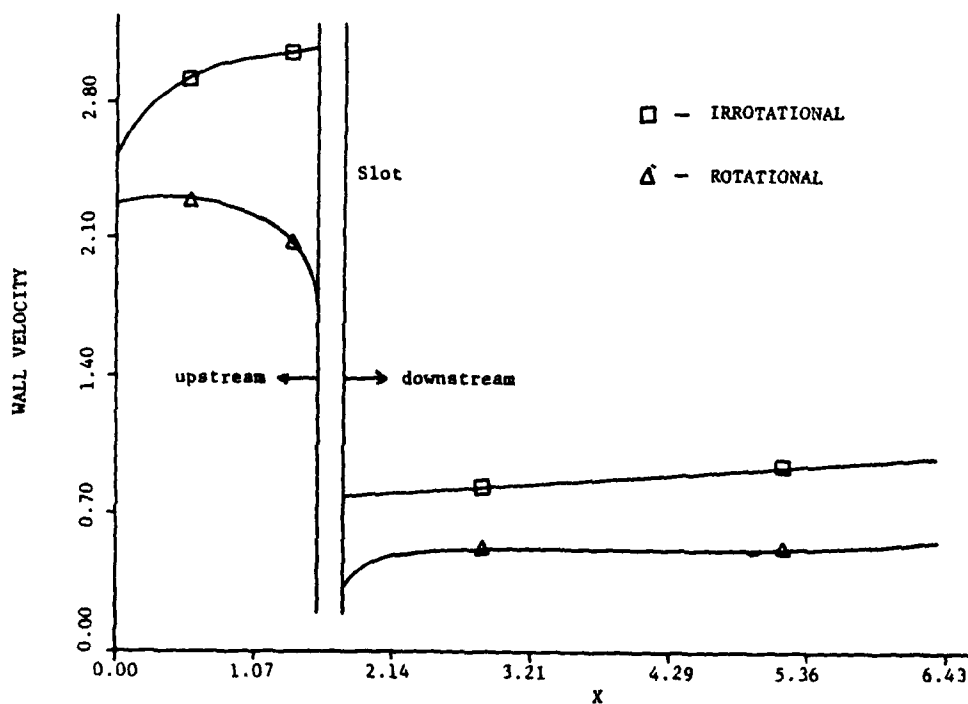

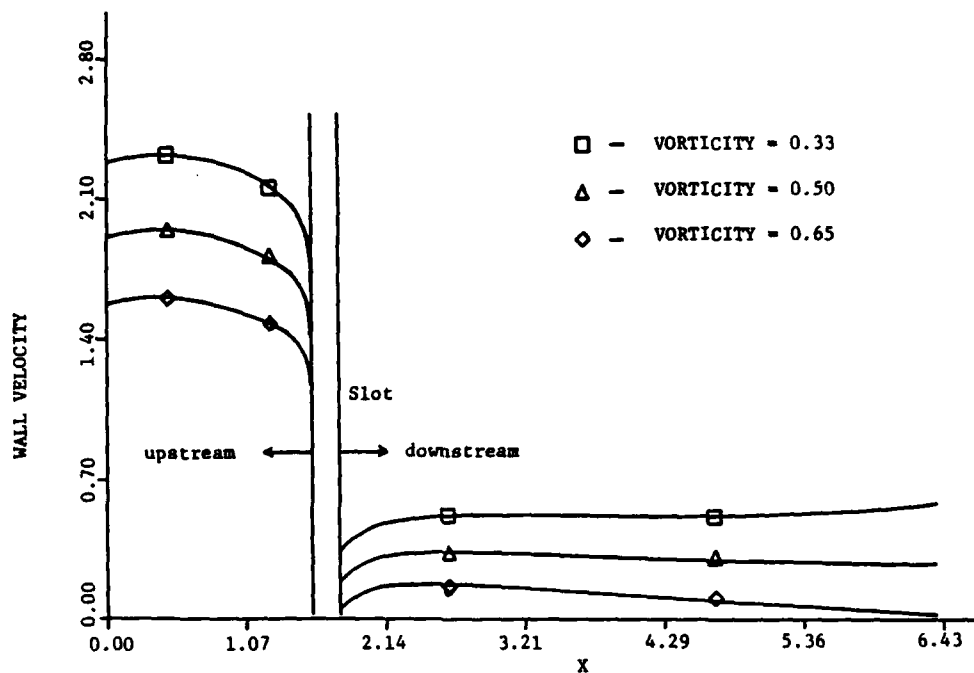Figure 12. Velocity distributions for rotational and irrotational flow.

34

Figure 13. Velocity distributions for three rotational flows with
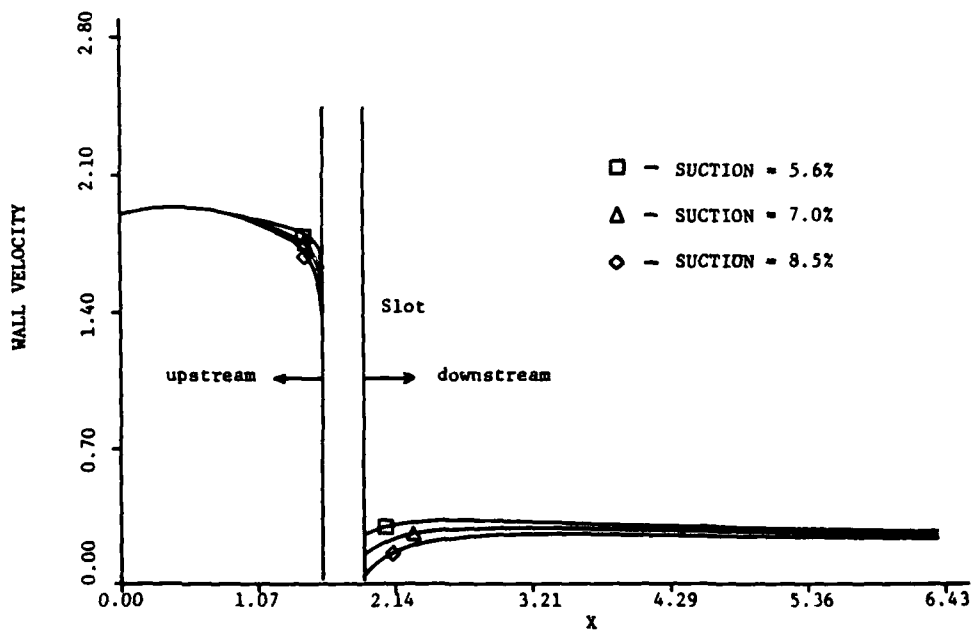suction rate of 5.6%.

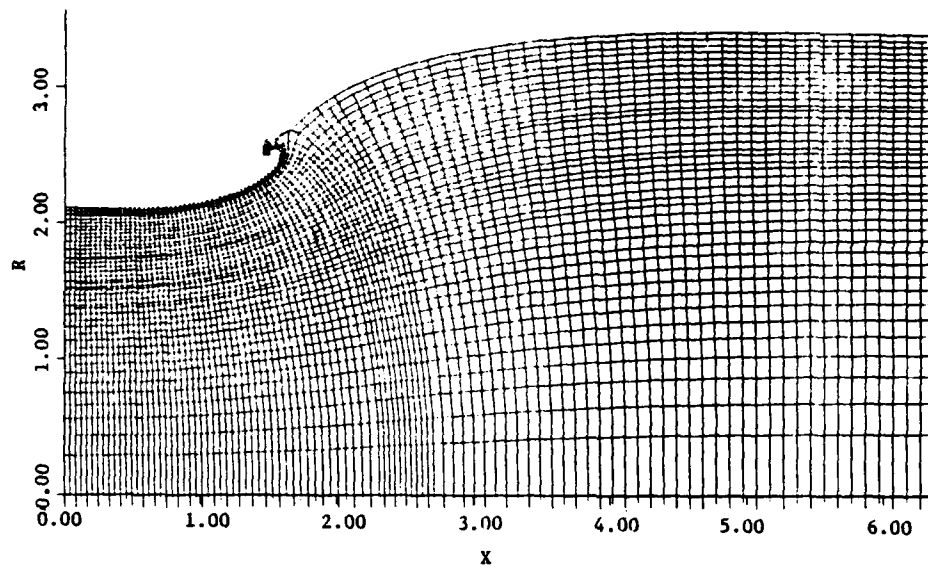Figure 14. Velocity distributions for rotational flow with B = 0.5 and
three suction rates.

35

Figure 15. Computer plot of $\phi - \psi$ grid for an axisymmetric diffuser, AR = 2.5, suction rate - 5.6% (Change in suction slot).
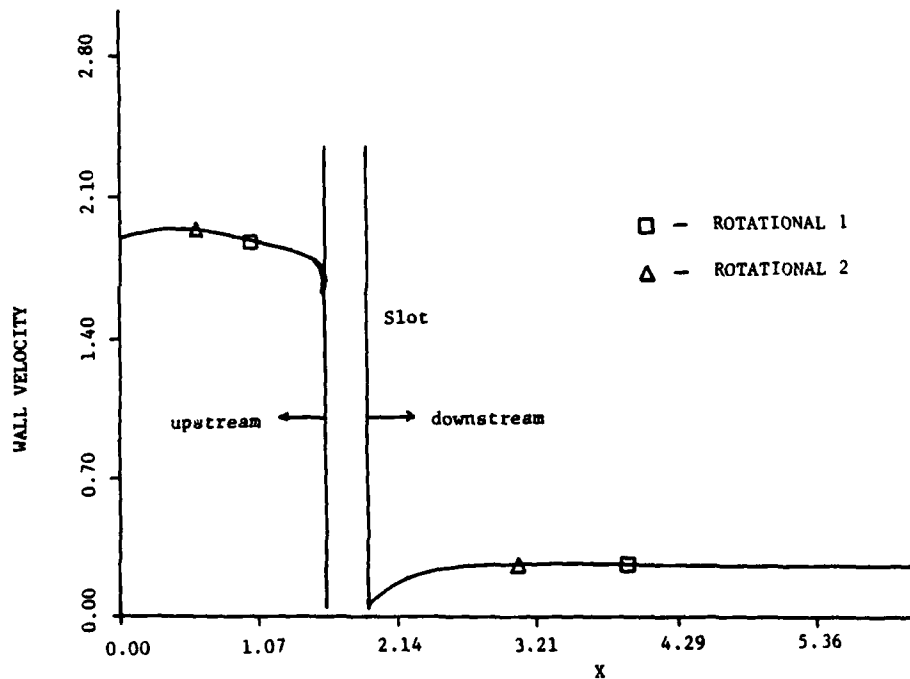

Figure 16. Velocity distributions for diffusers represented in Figures 11 and 15 (B = 0.5, suction rate = 8.5%).

36

Figure 17. Computer plot of $\phi - \psi$ grid for an axisymmetric diffuser, AR = 2.0, suction rate - 5.6%.

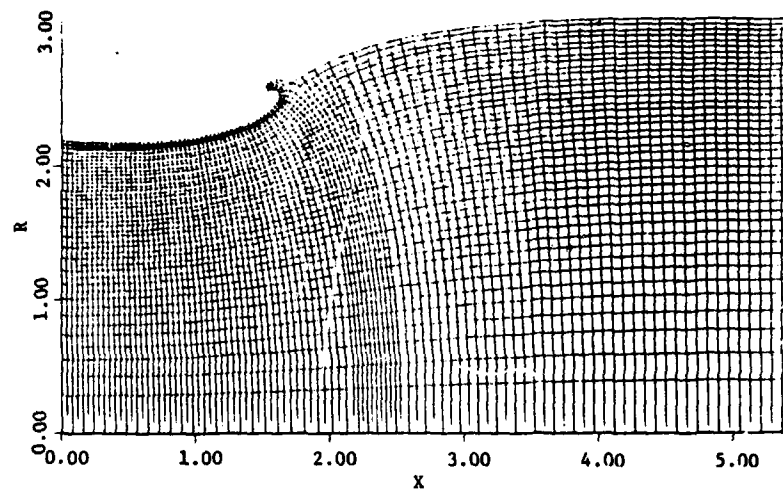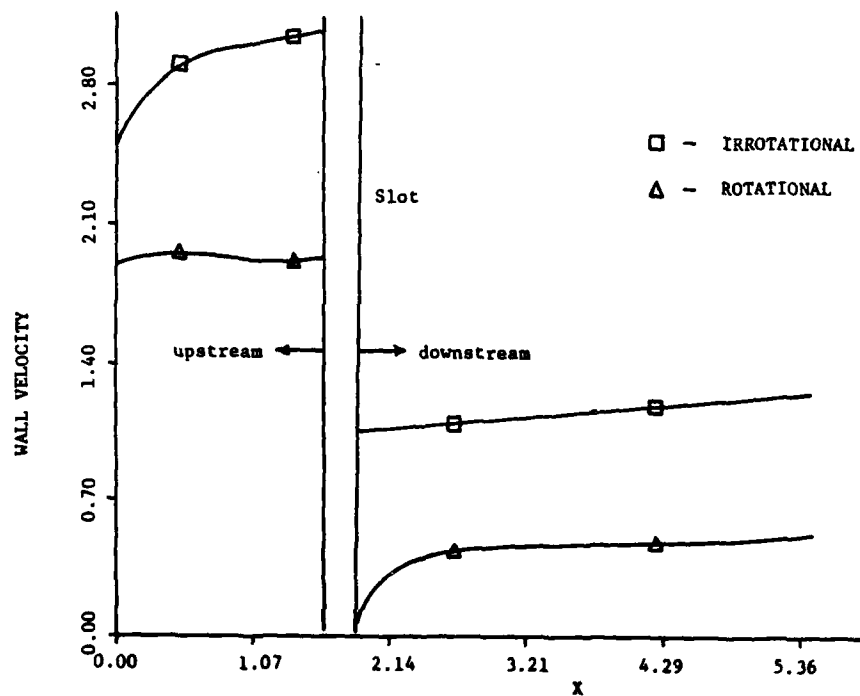Figure 18. Velocity distributions for rotational and irrotational flows, B = 0.5, suction rate = 8.5%.
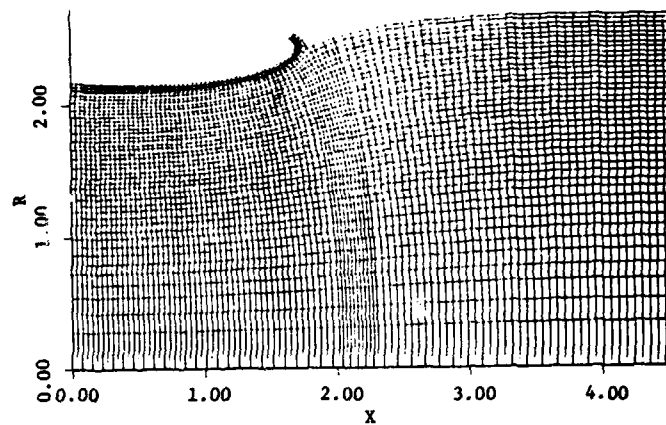
Figure 19. Computer plot of $\phi - \psi$ grid for an axisymmetric diffuser, AR = 1.5, suction rate = 8.5%.
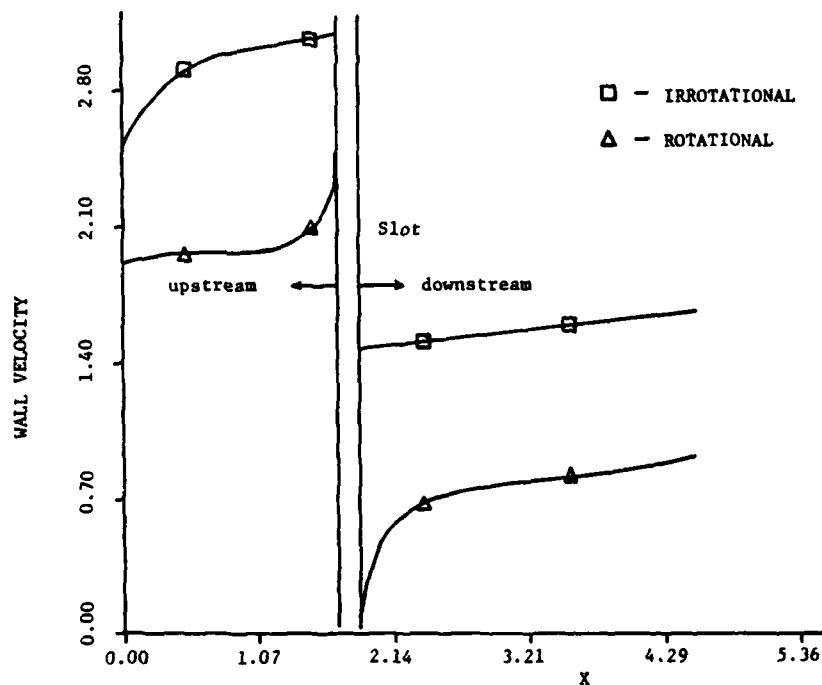
Figure 20. Velocity distributions for rotational and irrotational flows, B = 0.5, suction rate = 8.5%.
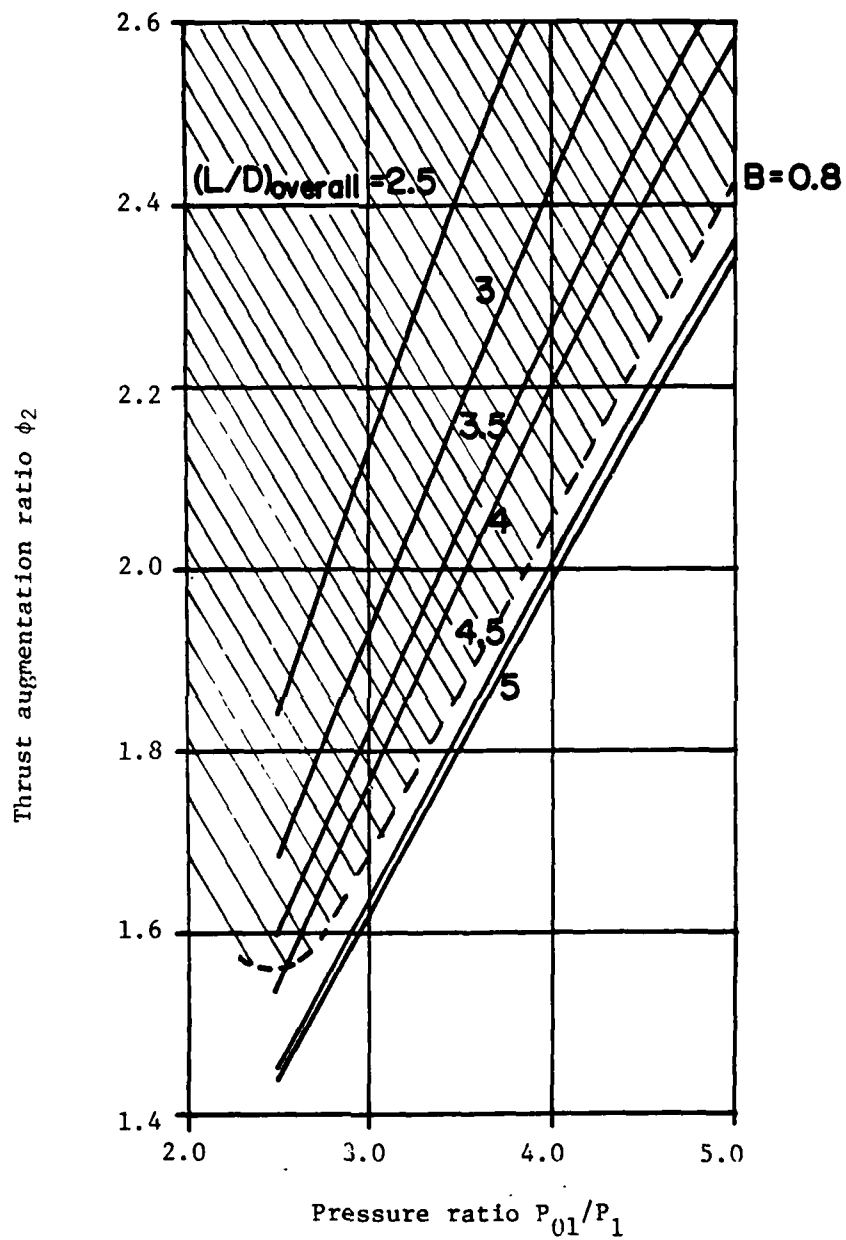
Figure 21.   Thrust augmentation ratio ϕ_2 vs. pressure ratio with $(L/D)_{overall}$ as parameter.
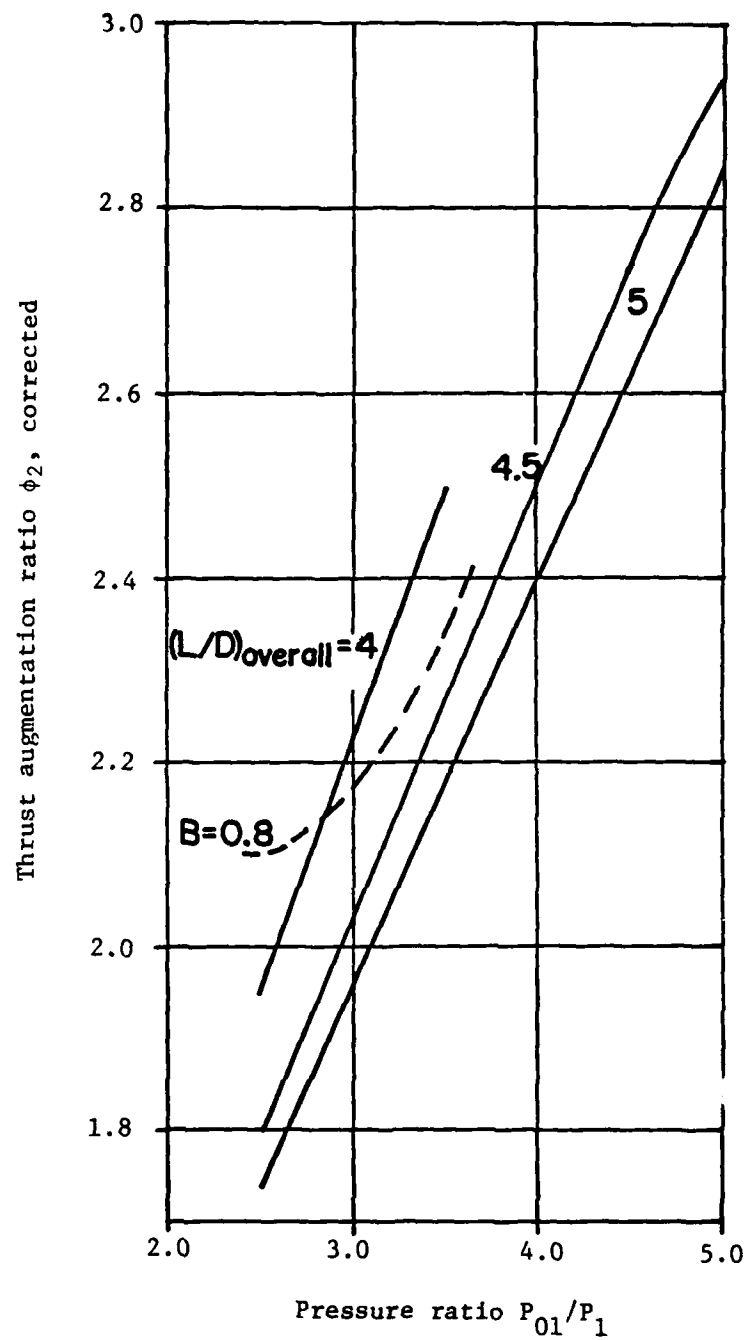
Figure 22. Corrected thrust augmentation ratio ϕ_2 vs. pressure ratio with $(L/D)_{overall}$ as parameter.

40
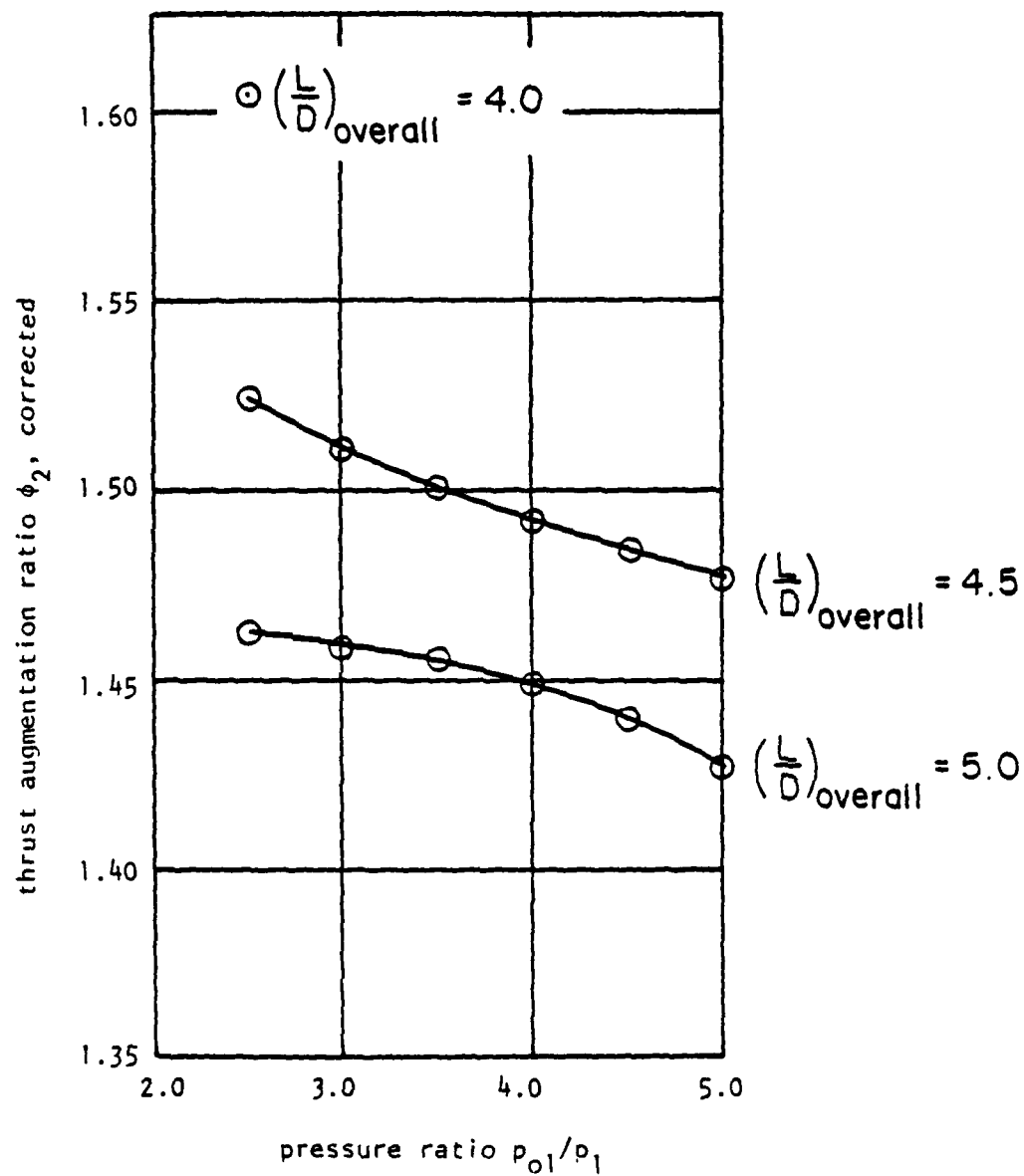
Figure 23. Corrected thrust augmentation ratio ϕ_2 vs pressure ratio with supersonic primary flows and with $(L/D)_{overall}$ as parameter.

41
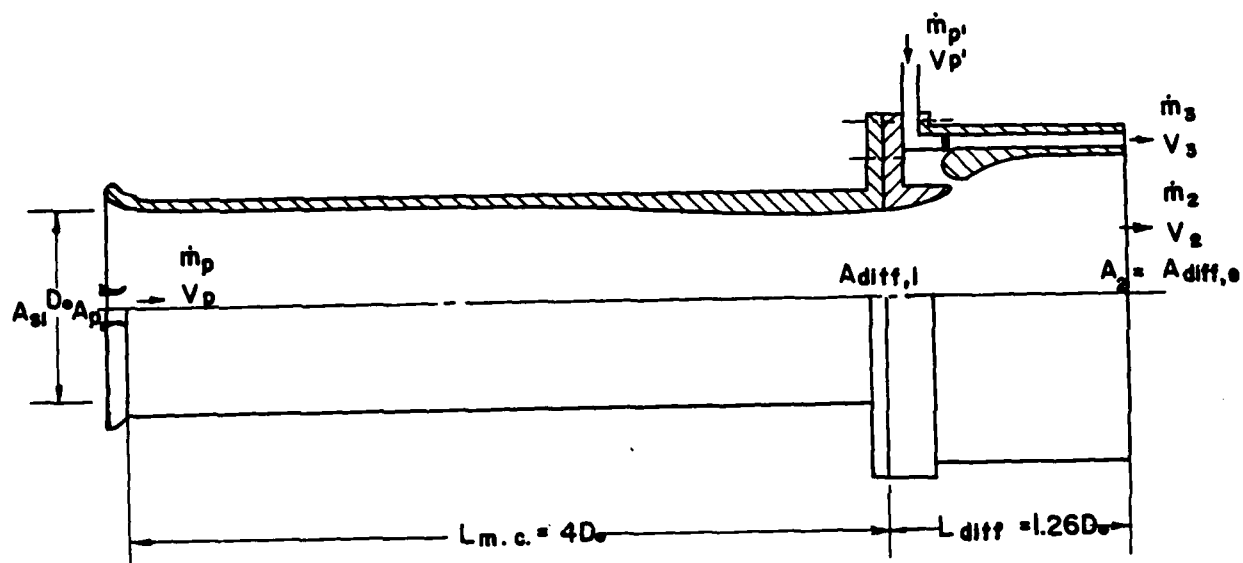
$$\frac{A_{\ell}}{A_{si}} = AR = 2 \qquad \frac{A_{diff,e}}{A_{diff,i}} = AR_{\ell} = 2.2 \qquad \phi_{\ell} = \frac{\dot{m}_{\ell}V_{\ell} + \dot{m}_3 V_3}{\dot{m}_p V_p + \dot{m}_{p'} V_{p'}} = 1.50$$

Figure 24.   Sample ejector (supersonic V_p and $V_{p'}$).

Figure 26. Thrust augmentation ratio ϕ_2 vs. percentage of contraction.

Figure 25. Boundary layer removal vs. percentage of contraction.

43

APPENDIX A

FLOW DIAGRAM AND INPUT INSTRUCTIONS
FOR DTNSRDC EJECTOR PROGRAM

44

APPENDIX A

In the DTNSRDC program, ejector inlet conditions are prescribed, as well
as the geometry of the mixing chamber of the ejector. The inlet conditions
are the relative dimensions of primary nozzle exit and mixing section inlet,
and the relative mass flow rates of the primary and secondary flows. The
prescribed geometry is used only up to the point of application of the
incipient separation criterion, corresponding to the diffuser inlet.

Figures A-1 and A-2 represent flow charts for the overall program and the
inner loop for the program. The inner loop contains a more involved iterative
procedure than was present in Gilbert and Hill's program; the pressure gradi-
ent in the diffuser section (REXO $\geq$ 0 or X $\geq$ XO) is adjusted iteratively to
meet the incipient separation criterion.

The program contains two termination tests:

1) If the number of iterations in the inner loop gets larger than 99 without
   the incipient separation criterion being satisfied, or if the friction
   velocity is negative at the end of the inner loop, abnormal ending of the
   calculations occur.

2) If the maximum length prescribed is reached or if atmospheric pressure is
   achieved, normal ending of the calculations occurs.

The following is the set of instructions for data input.

INSTRUCTIONS FOR DATA INPUT

Card No.	Parameters	Format
1	DP10, DP29, DP11	6E13.6
2	MK, NS, N, NJ, NK	815, 4F10.8
3		
4	PROFE(I), I - 1, MK	8F10.8
5		
6		
7	RRO(I), I = 1, NS	8F10.8
8		
9		
10	XXO(I), I = 1, NS	8F10.8
11		
12		
13	PSO(I), I = 53, 70	6E13.6
14		
15	NP, NPP, NL, NTEST, NJ, NM IPUNCH, KJ, SQP, CL, CU PERCNT	815, 4F10.8
16	PO1, TO1, PAMB, TOO, P1, YJIN, YJOU, RD	8F10.8
17	X, XX, XQ, REXO, CP2, CXX2, CA, B	8F10.8
18	NP, NPP, NL, NTEST, NJ, NM, IPUNCH, KJ, SQP, CL, CU, PERCNT	815, 4F10.8

Card 18 is the last card to end the calculations of the program, on which NPP must be set a value larger than 1.

Cards 1 through 17 are required for each set of data. For data more than one set, cards 1 through 19 must be placed in the same sequence.

MEANINGS OF SYMBOLS

DP10, DP20, DP11

Initial guessed pressure gradients on m = 1, 2 and zero lines respectively. The initial guesses of the values of DP10, DP20, DP11 at the initial plane may be assumed equal at any plus or minus dimensionless value of the order of 10^{-7} to 10^{-8}.

MK

A number which indicates the number of velocity and temperature detail being printed out.

NS

Indicates the total number of stations at which the geometry is given in sub-routine RADIUS.

N

Total number of streamlines.

NJ

Number of streamlines for primary flow.

NK

Number of streamlines for secondary flow, outside the boundary layer.

PROFE(I)

An array containing MK values of downstream positions in inches where the velocity and temperature details are required to be printed out.

BRO(I)

An array containing the total number (NS) of duct radius (inches).

XXO(I)

An array containing the total number NS of axial stations where the RRO(1)'s are provided (inches).

PSO(I)

Last 18 values of the non-dimensional stream function specified to satisfy the boundary layer requirements (see reference 1 for sample).

NP, NPP, NL, SQP

Control variables. For axisymmetric flow, NP = 2, NPP = 0, NL = 1, SQP = 0.5.

NTEST

Test run number.

CL, CU

Used in applying the incipient separation criterion. They are lower and upper limits to the dimensionless velocity at the last streamlines before the wall. CL = 0.0035 and CU = 0.0040 are representative values.

PO1

Nozzle plenum chamber pressure (PSIA).

TO1	Nozzle plenum chamber temperature ($^\circ$R).
PAMB	Ambient pressure (PSIA).
TOO	Ambient temperature ($^\circ$R).
P1	Pressure at nozzle exit (PSIA).
YJIN	Nozzle exit inner radius.
YJOU	Nozzle exit outer radius.
RD	Mixing section radius at inlet.
X	Distance from duct inlet to nozzle exit plane at which calculation begins (inches).
XX	Distance from duct inlet at which calculation stops.
XO	Distance from duct inlet at which incipient separation criterion is applied.
REXO	Control variable. Is negative for $X > XO$, positive for $X > XO$. Set REXO = -1 for input.
CP2	Gauge pressure (dimensionless) at diffuser exit. Set CP2 $\approx$ 0.
CXX2, CA, B	Parameters used in pressure gradient calculation for incipient separation criterion. Set CXX2 = 1.005, CA = 0.325, B = 1.

READ INITIAL CONDITIONS
AND INITIALIZE CONSTANTS

LAST DATA SET ────── STOP

NO   YES

CALL DST

CALL RADIUS

CALL PROF

CALL RTS

NSTEP=NSTEP+1

IS NSTEP=1

YES   NO

IS IFLOW=1

YES   NO

CALL LOOK

CALL EDDY

CALL STEP

U(2,N)=0; Y(1)=0

REXO ────── >0

≤0

CALL RADIUS   VOUT=Y(N)

CALCULATE UP

ICHX=0

INNER LOOP

X=X+ΔX

CALCULATE UV

IS NSTEP=1

NO   YES

IS NSTEP=1

NO   YES

NO   X > X₀ or REXO > 0   YES

PRINT X, Y(N), UE, AUGMENT, ETC.

ITER > 39 or UV < 0

YES   NO

REXO > 0

YES   NO

PRINT PROFILES AT SPECIFIED INTERVALS

NSTEP=1

YES   NO

CALL CHECK

CALL BLCHEK

REPLACE N=1 LINE VALUES WITH N=2 LINE VALUES

X > XX or UP > UPS

YES   NO

REXO > 0

YES   NO

(X - XO) < 0

CALCULATE AND PRINT CONDITIONS
AT DIFFUSER INLET

Figure A-1.   Flow Chart of DTNSRDC Computer Program

49

FROM MAIN

REXO

≤ 0 > 0

CALCULATE ΔP

CALL SOLU

ITER=ITER+1

ITER > 99

YES

NO

REXO < 0

YES

NO

U(2,69) < U69*.9 and U(2,69) $\geq$ CL

YES

NO

U(2,69) $\leq$ CU and U(2,69) $\geq$ CL

YES

NO

RECALCULATE A IF U(2,69) > CU
or U(2,69) < CL

STORE OLD VALUES OF y's, u's, o's
CALCULATE NEW o's, u's

CALL YDIS

REXO < 0

YES

NO

CALCULATE U#*

U#* > 0

YES

NO

A=0.95A

CALCULATE U#

U# > 1

YES

NO

A=0.95A

RESET NEW VALUES OF Y, U,
o EQUAL TO OLD STORED ONES

IS YOUT SATISFACTORY

NO   YES

CALL STAR

RESET NEW VALUES OF Y, U,
o EQUAL TO OLD STORED ONES
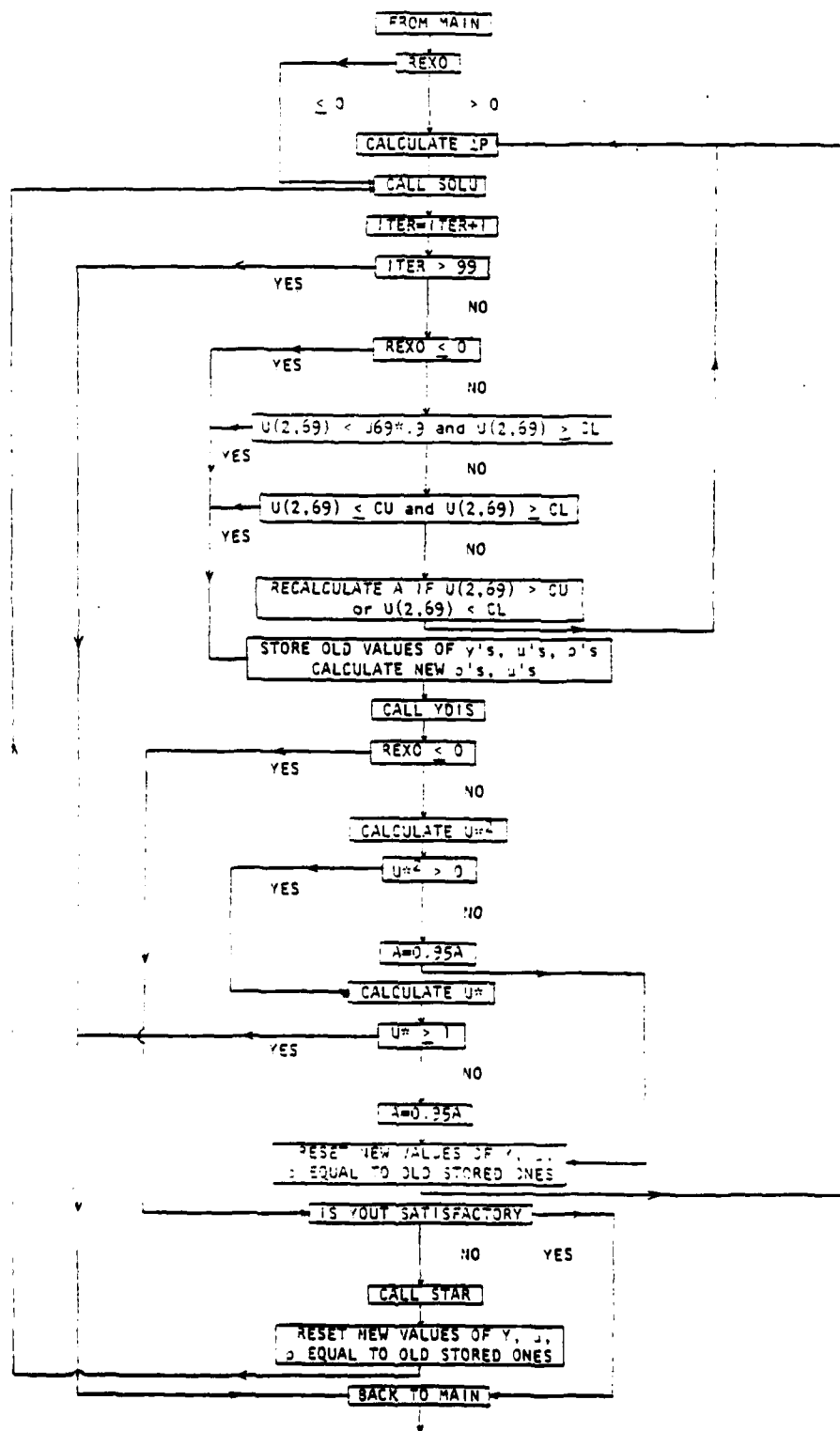
BACK TO MAIN

Figure A-2.   Inner Loop of DTNSRDC Computer Program

50

APPENDIX B

GLOBAL ANALYSIS FOR PARAMETRIC STUDY OF
THRUST AUGMENTING EJECTOR USING GRIFFITH DIFFUSER

Introduction

This analysis is conducted for the purpose of determining the ranges of operating parameters which will lead to a thrust ratio above 2.0 in an ejector for thrust augmentation. The thrust ratio is defined as the ratio of the exit momentum of the mixed fluid to the momentum of the primary fluid at the inlet.

In this study a special type of curved well diffuser, referred to as a Griffith Diffuser, is used. In order to operate the diffuser at a very high efficiency as it is intended, boundary layer control is necessary. Several auxiliary jets will be used to achieve the required boundary layer control. A parametric study was conducted in which net thrust rations were computed in addition to the thrust ratios defined above. The net thrust ratio is defined as the results of dividing the sum of exit thrust and pressure thrust minus the ram drag by the momentum of the primary flow. Upon examining the net thrust ratio one may see the relative contributions from the exit momentum terms and the pressure terms as well as the liability of the ram drag attributed by the momentum at the inlet of an ejector. Figure B1 shows a schematic diagram of the ejector for this study.
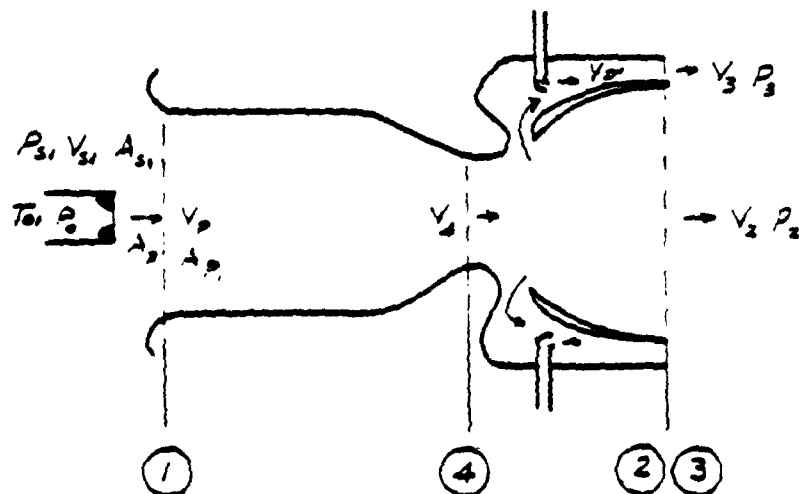

Figure B1. Schematic diagram of an ejector for thrust augmentation. Auxiliary jets are used for boundary layer control in diffuser.

$$(A_{pl} = A_p + A_p \quad A_{sl} = A_1 - A_p - \Delta A_p \quad \text{and} \quad \frac{A_p}{A_{sl}} = \frac{A_p}{A_1 - A_p})$$
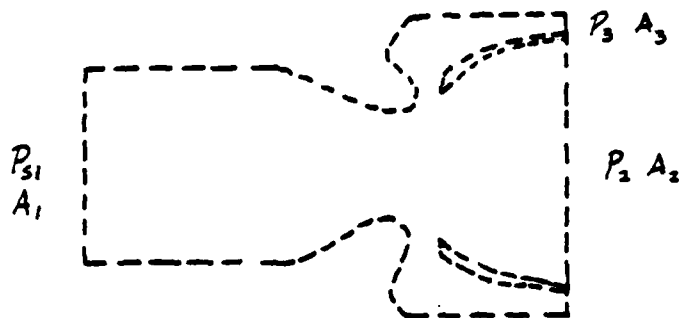
52

Figure B2. Control volume for momentum survey.

Analysis

Figure B2 shows a control volume from which the momentum equation for the fluid in x-direction is written as follows.

$$p_{p_1} A_{p_1} + p_{s_1} A_{s_1} - p_2 A_2 - p_3 A_3 + Th_{fx}$$

$$= \frac{1}{g_c} \left[\dot{m}_2 V_2 + \dot{m}_3 V_3 - \dot{m}_p V_p - \dot{m}_{s_1} V_{s_1} \right]$$

where Th_{fx} = force component in x-direction on the fluid at the interface of ejector and the fluid inside the control surface.

$$Th_{fx} = \frac{1}{g_c} \left[\dot{m}_2 V_2 + \dot{m}_3 V_3 - \dot{m}_p V_p - \dot{m}_{s_1} V_{s_1} \right]$$

$$- p_{p_1} A_{p_1} - p_{s_1} A_{s_1} + p_2 A_2 + p_3 A_3$$

The sum of force components in the x-direction on the ejector is denoted by Th_{ejx} and consists of the forces over the interior surface and exterior surface. The former is equal and opposite to Th_{fx}. Therefore, Th_{ej} = $- Th_{fx}$ + force components in x-direction on the exterior surface.

53

To find the force components in x-direction on the exterior surface of the ejector we may consider the following:
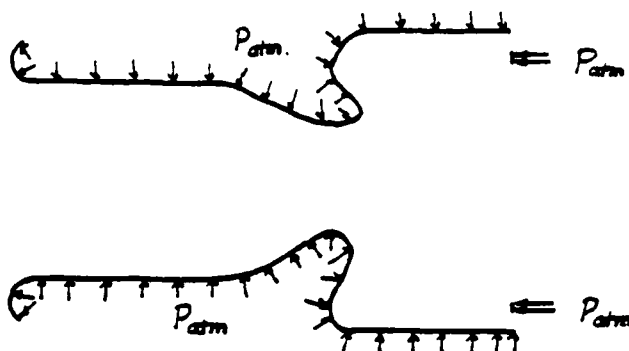

Figure B3. Exterior forces over the ejection.

Figure B3 shows the pressure force system over the exterior surface of the ejector and can be replaced by an equivalent of two sub-systems. Figure B4 shows the sub-systems.
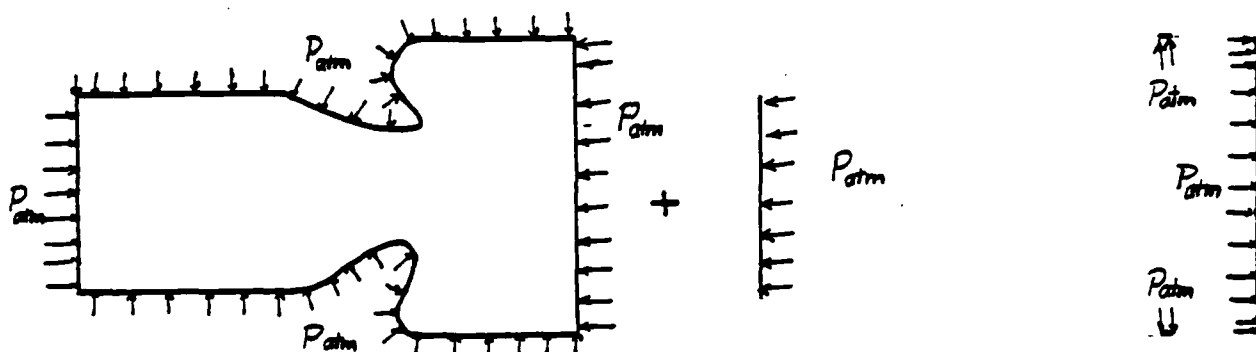

Figure B4. An equivalent force system made up of two sub-systems.

The left-hand side sub-system has a resultant of zero, therefore the force system represents the exterior pressure force, shown as Figure B3, can be replaced by the right-hand side of the sub-system of Figure B4 or

$$Th_{ejx} = - p_{atm} A + p_{atm} A_3 + p_{atm} A_2 + p_{p_1} A_{p_1} + p_{s_1} A_{s_1}$$

$$- p_2 A_2 - p_3 A_3 - \frac{1}{g_c} [\dot{m}_2 V_2 + \dot{m}_3 V_3 - \dot{m}_p V_p - \dot{m}_{s_1} V_{s_1}]$$

Since p_2 and p_3 are the ambient pressure, we have $p_2 = p_3 = p_{atm}$. In addition,

$$A_1 = A_{s_1} + A_{p_1}.$$

54

Therefore,

$$Th_{ejx} = -p_{atm} (A_{s_1} + A_{p_1}) + p_{p_1} A_{p_1} + p_{s_1} A_{s_1}$$

$$- \frac{1}{g_c} [\dot{m}_2 V_2 + \dot{m}_3 V_3 - \dot{m}_p V_p - \dot{m}_{s_1} V_{s_1}]$$

Since the primary jet is placed away from the inlet of the mixing chamber, we have $p_{p_1} = p_{s_1}$

Therefore,

$$Th_{ejx} = (p_s - p_{atm}) A_1 - \frac{1}{g_c} (\dot{m}_2 V_2 + \dot{m}_3 V_3) + \frac{1}{g_c} (\dot{m}_p V_p + \dot{m}_{s_1} V_{s_1}).$$

In this equation, $(p_{s_1} - p_{atm})$ is the gage pressure at the mixing chamber inlet and is a negative quantity and contributes positively to the thrust on the ejector. We refer to this as pressure thrust. The term $[-\frac{1}{g_c} (\dot{m}_2 V_2 + \dot{m}_3 V_3)]$ is the exit thrust force that also contributes positively to the thrust on the ejector. The last term, $[(\frac{1}{g_c} (\dot{m}_p V_p + \dot{m}_{s_1} V_{s_1})]$ is the ram drag, a liability to the thrust of the ejector. If the primary jet is located inside the mixing chamber inlet, then the condition $p_{p_1} = p_{s_1}$ may not hold.

In a single thrust augmentor, the thrust ratio is usually denoted by and is defined as follows:

$$\phi = \frac{\dot{m}_2 V_2}{\dot{m}_p V_p}$$

In the system described in this analysis we use the symbol ϕ_2 for thrust ratio, and this is defined as follows

$$\phi_2 = \frac{\dot{m}_2 V_2 + \dot{m}_3 V_3}{\dot{m}_p V_p + \dot{m}_{p'} V_{p'}}$$

where $\dot{m}_{p'}$ and $V_{p'}$ denote the mean flow rate and jet velocity, respectively, of the auxilliary jets used in the diffuser for boundary layer control.

55

The net thrust ratio then is denoted by TR, and

$$TR = \frac{Th_{ejx}}{(\dot{m}_p V_p + \dot{m}_{p'} V_{p'})} \frac{1}{g_c}$$

$$+ \frac{-(\dot{m}_2 V_2 + \dot{m}_3 V_3) + \dot{m}_p V_p + \dot{m}_{s_1} V_{s_1} + (p_{s_1})_{gage} A_1 g_c}{\dot{m}_p V_p + \dot{m}_{p'} V_{p'}}$$

For convenience we introduce the following symbols:

$$MR = \text{mass ratio} = \frac{\dot{m}_{s_1}}{\dot{m}_p} \quad \text{and} \quad MR_p = \frac{\dot{m}_{p'}}{\dot{m}_p}$$

Then

$$\dot{m}_{s_1} = MR \, \dot{m}_p \quad \text{and}$$

$$\dot{m}_2 = (1 - FS)(MR + 1)\dot{m}_p$$

where FS stands for fraction of through flow sucked away for the purpose of boundary layer control in the diffuser, and

$$\dot{m}_3 = \dot{m}_{p'} + FS \, (MR + 1) \, \dot{m}_p .$$

It can be shown that the net thrust ratio TR can be expressed as follows.

$$TR = \frac{-(1 - FS)(MR + 1)V_2 - MR_p V_3 - FS \, (MR + 1)V_3}{V_p + MR_p V_{p'}}$$

(exit thrust ratio)

$$+ \frac{(p_{s_1})_{gage} \quad A_1 \frac{g_c}{\dot{m}_p}}{V_p + MR_p V_{p'}} \qquad + \qquad \frac{V_p + MR \, V_{s_1}}{V_p + MR_p V_{p'}}$$

(pressure thrust ratio)   (ram drag ratio)

56

Introducing PR, the absolute pressure ratio of nozzle plenum to secondary flow at the mixing chamber inlet

$$PR = \frac{P_{o,a}}{P_{sl,a}}$$

Then $(p_{sl})_{gage} = \dfrac{P_{o,a}}{PR} - P_{atm}$

and

$$TR = \frac{V_p + (MR)\, V_s}{V_p + (MR)_p\, V_{p'}} + \frac{\left(\dfrac{P_{o,a}}{PR} - P_{atm}\right)\left(1 + \dfrac{A_s}{A_p}\,\dfrac{g_c}{\rho_p\, V_p}\right)}{V_p + (MR)_p\, V_{p'}} - p_2$$

Geometrical and Flow Parameters

The ratio of the secondary flow area at the ejector inlet to that of

the primary jet, $\dfrac{A_{sl}}{A_p}$, and the diffuser area ratio, $(AR)_{diff}$, are

specified geometrically. The mixing chamber geometry, however, at this stage of the study will not be specified directly. For each mixing chamber along with other parts of the ejector under a particular set of operating conditons (namely the plenum pressure of the primary jet $P_{o,a}$ and the discharge pressures P_2 and P_3), there is a specific velocity profile within the boundary layer upstream of the suction slot of the diffuser. This specific boundary layer implies a specific value of FS, the fraction of suction, and a specific value of mass ratio MR. Therefore we will assign a range of values for FS and MR respectively to suggest that different mixing chambers are involved.

Similarly we will assign several values of MR_p, the ratio of mass flow rate in the primary jet to that in the auxiliary jets, instead of specific geometrical details of the auxiliary jets. Alternatively $(MR)_{aux}$, the ratio of entrained mass flow rate to the mass flow rate in the jets of the auxiliary ejector, for boundary layer control may be

57

introduced and MR_p calculated from $(MR)_{aux}$ and other parameters. Specifying $(MR)_{aux}$ along with MR provides a relative performance description between the primary ejector and the auxiliary ejector.

Once the above parameters are specified, all the variables involved in computing ϕ_2 and TR can be determined from the following equations.

1. V_p:

$$V_p = 2g_c \, J \, \eta_N \, C_p \, T_o \left[1 - \frac{p_{p,a}}{p_{o,a}}^{\frac{k-1}{k}} \right]^{\frac{1}{2}}$$

where η_N is the nozzle efficiency, and is assumed to be 0.95

C_p is the specific heat at constant pressure for air

k is the ratio of specific heats

$p_{p,a}$ is either the atmospheric pressure or the critical pressure, $0.5283 \, P_{o,a}$

$P_{o,a}$ is previously defined and is specified

T_o is air temperature inside the nozzle plenum

2. ρ_p:

$$\rho_p = \frac{p_{p,a}}{R T_{pa}} = \frac{p_{p,a}}{R \, T_o \, \frac{p_{p,a}}{p_{o,a}} \frac{k-1}{k}}$$

where R is the gas constant

3. V_{s_1}:

From $\dot{m}_s = MR \, \dot{m}_p$

$$(\rho \, A \, V)_{s_1} = MR \, (\rho \, A \, V)_p$$

$$V_{s_1} = MR \, \frac{\rho_p}{\rho_{s_1}} \, \frac{A_p}{A_{s_1}} \, V_p$$

$$= (MR) \, (DR) \, \left(\frac{1}{\lambda}\right) V_p$$

58

where $DR = \dfrac{P_{atm}}{T_{atm}} \left[\dfrac{P_{p,a}}{P_{o,a}} \right]^{\frac{k-1}{k}}$

$$\lambda = \dfrac{A_{s1}}{A_p}$$

4. $(P_s)_{gage}$:

$$(P_s)_{gage} = \dfrac{V_{s1}^2 \, \rho_{s1}}{2g_c}$$

5. $V_{p'}$:

$$V_{p'} = \left[2g_c \, J \, \eta_N \, C_p \, T_o \left[1 - \dfrac{P_{p',a}}{P_{o,a}} \right]^{\frac{k-1}{k}} \right]^{\frac{1}{2}}$$

For the range of $P_{o,a}$ to be considered

$P_p = P_{p'} = P_{critical}$

Therefore, $V_p = V_{p'}$

6. MR_p:

$$MR_p = \dfrac{\dot{m}_p}{\dot{m}_p} = \dfrac{\rho_{p'} \, A_{p'} \, V_{p'}}{\rho_p \, A_p \, V_p} = \dfrac{A_{p'}}{A_p}$$

7. $(MR)_{aux}$:

$$\dot{m}_{p'} \, (MR)_{aux} = F.S. \, (MR + 1)\dot{m}_p$$

$$(MR)_{aux} = \dfrac{F.S. \, (MR + 1)}{MR_p}$$

59

8. V_2:

$$(\rho AV)_2 = (\dot{m}_{s_1} + \dot{m}_p)(1 - F.S.) = (MR + 1)(1 - F.S.)\dot{m}_p$$

$$\therefore V_2 = \frac{(MR + 1)(1 - F.S.) \rho_p A_p V_p}{(AR) A_1 \rho_2}$$

where ρ_2 is at T_2 and P_2 corresponding to standard atmospheric conditions.

9. V_3:

$$(\dot{m}_3 V_3)_x = (\dot{m}_{p'} V_{p'})_x$$

where the subscript x denotes x-direction

and $\dot{m}_3 = F.S.$ $(MR + 1)$ $\dot{m}_p + \dot{m}_{p'}$

$$\therefore V_3 = \frac{(MR)_p}{F.S. (MR + 1) + MR_p} V_{p'}$$

Range of Values Used in Parametric Study

1. $A_p = 0.0013$ ft^2
2. $\lambda = \dfrac{A_{s1}}{A_p} = 103.9, 176.3$
3. $AR = 1.0, 1.25, 1.50$
4. $F.S. = 0.05, 0.10, 0.15$
5. $MR = 10, 13, 16, 19, 22, 25$
6. $(MR)_{aux} = 5, 7.5$
7. $(P_o) = 35, 43.75, 52.5, 61.25, 70$ (PSIA)

60

Results: One thousand and eighty (1080) TR and ϕ_2 were computed. 68% of the 1080 runs led to ϕ_2 above 2.0. The results of this analysis ponts out the necessary levels of performances for MR and $(MR)_{aux}$ and th restrictions on boundary layer development in the mixing chamber required to achieve a thrust ratio above 2.0.

DATE
ILMED

8